Animal 18 (2024) 101269

Contents lists available at ScienceDirect

Animal
The international journal of animal biosciences

Kinematic changes in dairy cows with induced hindlimb lameness: transferring methodology from the field of equine biomechanics

A. Leclercq [a,*], K. Ask [a], Y. Mellbin [a], A. Byström [b], F.M. Serra Bragança [c], M. Söderlind [a], E. Telezhenko [d], C. Bergsten [e], P. Haubro Andersen [a], M. Rhodin [a], E. Hernlund [a]

[a] Department of Animal Biosciences, Swedish University of Agricultural Sciences, Uppsala, Sweden
[b] Department of Applied Animal Science and Welfare, Swedish University of Agricultural Sciences, Uppsala, Sweden
[c] Department of Clinical Sciences, Utrecht University, Utrecht, the Netherlands
[d] Department of Biosystems and Technology, Swedish University of Agricultural Sciences, Alnarp, Sweden
[e] Department of Clinical Sciences, Swedish University of Agricultural Sciences, Uppsala, Sweden

ARTICLE INFO

Article history:
Received 17 November 2023
Revised 12 July 2024
Accepted 16 July 2024
Available online 22 July 2024

Keywords:
Biomechanics
Bovine
Gait analysis
Inertial measurement unit
Lameness detection

ABSTRACT

Lameness is a common issue on dairy farms, with serious implications for economy and animal welfare. Affected animals may be overlooked until their condition becomes severe. Thus, improved lameness detection methods are needed. In this study, we describe kinematic changes in dairy cows with induced, mild to moderate hindlimb lameness in detail using a "whole-body approach". Thereby, we aimed to identify explicable features to discriminate between lame and non-lame animals for use in future automated surveillance systems. For this purpose, we induced a mild to moderate and fully reversible hindlimb lameness in 16 dairy cows. We obtained 41 straight-line walk measurements (containing > 3 000 stride cycles) using 11 inertial measurement units attached to predefined locations on the cows' upper body and limbs. One baseline and ≥ 1 induction measurement(s) were obtained from each cow. Thirty-one spatial and temporal parameters related to limb movement and inter-limb coordination, upper body vertical displacement symmetry and range of motion (**ROMz**), as well as pelvic pitch and roll, were calculated on a stride-by-stride basis. For upper body locations, vertical within-stride movement asymmetry was investigated both by calculating within-stride differences between local extrema, and by a signal decomposition approach. For each parameter, the baseline condition was compared with induction condition in linear mixed−effect models, while accounting for stride duration. Significant difference between baseline and induction condition was seen for 23 out of 31 kinematic parameters. Lameness induction was associated with decreased maximum protraction (−5.8%) and retraction (−3.7%) angles of the distal portion of the induced/non-induced limb respectively. Diagonal and lateral dissociation of foot placement (ratio of stride duration) involving the non-induced limb decreased by 8.8 and 4.4%, while diagonal dissociation involving the induced limb increased by 7.7%. Increased within-stride vertical displacement asymmetry of the poll, neck, withers, thoracolumbar junction (back) and *tubera sacrale* (**TS**) were seen. This was most notable for the back and poll, where a 40 and 24% increase of the first harmonic amplitude (asymmetric component) and 27 and 14% decrease of the second harmonic amplitude (symmetric component) of vertical displacement were seen. ROMz increased in all these landmarks except for TS. Changes in pelvic roll main components, but not in the range of motion of either pitch or roll angle per stride, were seen. Thus, we identified several kinematic features which may be used in future surveillance systems. Further studies are needed to determine their usefulness in realistic conditions, and to implement methods on farms.
© 2024 The Authors. Published by Elsevier B.V. on behalf of The Animal Consortium. This is an open access article under the CC BY license (http://creativecommons.org/licenses/by/4.0/).

Implications

Lameness is common in dairy cows, and better detection methods are needed so that animals can receive timely treatment. In this study, the movements of walking cows with induced lameness

* Corresponding author.
E-mail address: anna.leclercq@slu.se (A. Leclercq).

https://doi.org/10.1016/j.animal.2024.101269
1751-7311/© 2024 The Authors. Published by Elsevier B.V. on behalf of The Animal Consortium.
This is an open access article under the CC BY license (http://creativecommons.org/licenses/by/4.0/).

were measured using inertial measurement units, which were attached to the animal. Different measures were then calculated and compared between lame and non-lame animals. Although more studies are needed, our results indicate that this method may be useful for implementation in future automatic lameness detection systems, which potentially could contribute to earlier discrimination between lame and non-lame animals, and thereby improved welfare and increased societal acceptance of keeping of cows.

Introduction

Lameness caused by claw disorders is a common problem in dairy herds with well-documented negative consequences for economy and productivity (Leach et al., 2010; Cha et al., 2010; O'Connor et al., 2023) as well as animal welfare (Ventura et al., 2015). Thus, prompt detection and treatment of claw disorders are essential in order to minimise these effects. However, growing herd sizes render visual lameness detection more difficult.

Traditionally, lameness in dairy cows is detected by visual assessment performed by e.g. animal caretakers or specifically trained personnel. In the current literature, there are several descriptions of visual scales intended to facilitate lameness assessment (Schlageter-Tello et al., 2014b; Van Nuffel et al., 2015b). Previously described scales rely on the assessment of e.g. back shape, head bob, joint flexion, and step length (Sprecher et al., 1997; Flower and Weary, 2006; Agriculture and Horticulture Development Board, 2023). However, visual lameness detection can be complicated and time−consuming. In one previous study, the prevalence of lameness (as judged by the researchers) was 3.1 times higher than the farmer-estimated prevalence (Espejo et al., 2006), indicating that farmers underestimate the prevalence of lameness in their herds. Moreover, gait alterations are often not discovered until they have become severe (Espejo et al., 2006; Leach et al., 2010). In addition to the difficulties in spotting lame individuals in large herds, visual lameness detection is prone to observer bias, meaning that different observers may have different opinions regarding the lameness degree of the same individual. In cows, varying degrees of consistency in subjective lameness assessment have been demonstrated (Winckler and Willen, 2001; Engel et al., 2003; Flower and Weary, 2006; Schlageter-Tello et al., 2014a).

In an attempt to increase the efficiency in early lameness detection, a lot of work has been conducted with the aim of developing automatic lameness detection methods for dairy cows (e.g. Thorup et al., 2014; Lorenzini et al., 2017; Kang et al., 2020). Methods described in previous research include use of accelerometers (Alsaaod et al., 2017; O'Leary et al., 2020), inertial measurement units (**IMUs**) (Haladjian et al., 2018), pressure-sensitive mats (Van Nuffel et al., 2015a), force plates (Mokaram Ghotoorlar et al., 2012) and recording of the back shape using 3D cameras (Viazzi et al., 2013). In later years, major advancements in the field of computer vision have been made, which provides new possibilities as objective gait assessment without the need for markers and/or sensors is enabled (Kang et al., 2020; Russello et al., 2022; Barney et al., 2023).

Despite extensive research, lameness is still common in dairy cows, with mean prevalence of lameness as high as 22.8% (Thomsen et al., 2023) reported. It remains a challenge to detect mild cases of lameness. However, decreased productivity in dairy cows is seen already at an early stage of disease (Green et al., 2002; O'Connor et al., 2023). Importantly, a shorter time between onset and treatment of claw disorders reduces the need for follow-up treatments and lowers the prevalence of lameness at herd level (Leach et al., 2012). Thus, continued development towards earlier detection of lameness is needed to reduce production loss and improve animal welfare.

A detailed understanding of kinematic changes associated with lameness is currently lacking in cattle. From a biomechanical point of view, the horse is a much more studied species (Nejati et al., 2023). A number of IMU-based systems for gait analysis, which quantify within-stride, or "between-stride half/between-step" differences in upper body segment displacement, are now commercially available and used in equine clinics (Serra Bragança et al., 2018; Crecan and Peştean, 2023). These methods' potentials as lameness assessment tools in cows are yet to be explored. Being quadrupedal−hoofed animals, cattle and horses share important anatomical features, but commonly suffer from different orthopaedic pathologies (Bergsten, 1994; Penell et al., 2005). Moreover, they are normally assessed at different gaits (walk and trot respectively). Although lameness-induced kinematic changes should therefore not be expected to be identical in the two species, lameness generally implies load redistribution between limbs, where the maximum load accepted by the painful limb(s) is reduced (Scott, 1989; Buchner et al., 1996). In horses, it is known that this is reflected as decreased within-stride symmetry in the movement of upper body segments (Buchner et al., 1996). In cows, "uneven gait" (Winckler and Willen, 2001) and "uneven head movement" (Flower and Weary, 2006), are (subjectively) described as signs of lameness also in cows. Although asymmetry of limb kinematics has been objectively described in lame cows (e.g. Maertens et al., 2011, Alsaaod et al., 2017), within-stride asymmetry of upper body movement has received less attention.

Knowledge from the field of equine biomechanics may thus inspire studies within bovine biomechanics, where methodological adaptations to the bovine species and the walking gait are made. For example, as the walk is a more complex gait than trot involving both diagonal and lateral bipedal, as well as tripedal support phases (Hildebrand, 1989), changes in inter-limb coordination may be of greater importance than in trot. Using elaborate signal processing approaches, the raw acceleration and angular velocity signals obtained from IMU-based gait analysis systems can be integrated into displacement and angle data (Pfau et al., 2005; Bosch et al., 2018). Using limb-mounted IMUs, foot-on moments of each limb can be detected (Serra Bragança et al., 2017), and thus also temporal measures can be computed on a stride-by-stride basis. In horses, assessment of within-stride asymmetries of head and trunk vertical displacement is commonly used due to its robustness in detecting weight-bearing lameness and determining the affected limb at trot (Buchner et al., 1996; Keegan et al., 2003; Persson-Sjodin et al., 2023). Asymmetry of upper body vertical displacement can be quantified by calculating within-stride differences between local extrema of the vertical displacement signal (Bosch et al., 2018) or by employing signal decomposition approaches (Peham and Scheidl, 1996; Keegan et al., 2001; Audigié et al., 2002). Further, spatial and temporal characteristics of limb motion can be considered in conjunction with parameters relating to upper body kinematics, and contribute to a more comprehensive view of movement pattern alterations associated with lameness.

In this study, we aimed to identify and describe important kinematic features associated with hindlimb lameness in dairy cows by applying adapted knowledge from the field of equine biomechanics. A reversible lameness induction method was employed, which enabled us to study unilateral, mild to moderate hindlimb lameness while accounting for inter-individual variability. With the use of 11 upper body- and limb-mounted IMUs, 31 kinematic measures were obtained, in each subject, before and after lameness induction. Thereby, we aimed to contribute with detailed and comprehensible knowledge on kinematic gait changes during lameness at walk−in cattle, to advance the development of objective lame-

ness detection systems. We hypothesised that induction of lameness would cause increased within-stride asymmetry, both for upper body and limb kinematic parameters.

Material and methods

Animals

Seventeen first- or second−parity, milk-producing dairy cows (Swedish Red: N = 8, Holstein: N = 9), housed at the Swedish Livestock Research Centre at Lövsta, Swedish University of Agricultural Sciences, Uppsala, Sweden, were initially selected for the study. Average days in milk was 125 days (range: 31–281 days). Just before her first measurement, each cow was clinically examined by a veterinarian, to rule out ongoing disease (i.e. rectal temperature, rumen motility, heart rate and respiration rate were checked and confirmed to be within normal ranges, all limbs as well as the udder were inspected and palpated to confirm absence of notable lesions). All cows' claws were trimmed according to the five-step Dutch method (Toussaint-Raven et al., 1989) and examined for absence of severe claw lesions by an experienced claw trimmer, no longer than 3 months prior to data collection. Only mild dermatitis to the interdigital skin and mild sole haemorrhages (Egger-Danner et al., 2015) were deemed acceptable findings. All animals were free from obvious conformational deviations, and no cows had udders that extended below the level of the hock joint.

Experimental setup and data collection

All experimental procedures, which were also partly described in (Tijssen et al., 2021), were carried out at the Swedish Livestock Centre at Lövsta, Uppsala, Sweden. All measurements were performed in a free stall pen with a straight, 72 m long and 2 m wide measurement aisle with diamond-pattern grooved, solid concrete floor. Prior to measurements, two cows were brought to the pen simultaneously and were allowed to habituate to the surroundings. The cows' gait was then measured in the aisle using the equine gait analysis system Equimoves (Netherlands) (Bosch et al., 2018; Inertia Technology n.d.), as already described (Tijssen et al., 2021). Every cow was equipped with 11 IMUs (ProMove, Inertia-Technology B.V., Enschede) attached to the following pre defined upper body and limb landmarks: the middle of the poll (poll), on the right side of the neck collar (neck), between the shoulder blades (withers), at the thoracolumbar junction (back), left and right *tuber coxae* (**LTC** and **RTC**), between the *tubera sacrale* (**TS**), and laterally on each limb, on the mid-metacarpus and metatarsus, respectively (left front = **LF**, right front = **RF**, left hind = **LH**, right hind = **RH**). The upper body IMUs (i.e. all except the limb IMUs) were placed in custom-made cases, and glued to the cow using cyanoacrylate glue (36-2375, Biltema, Sweden). Before removal, the glue was dissolved using 100% acetone. The neck IMU was attached to the collar using adhesive tape, and the limb IMUs were attached using custom-made straps. See (Tijssen et al., 2021) and Fig. 1 for visualisation of IMU placement.

The upper body IMUs had two triaxial accelerometers, one with a range of ± 8 g for measuring low-g acceleration and one ± 100 g for measuring high-g acceleration, and a triaxial gyroscope with a range of ± 2 000 degrees/s for measuring angular velocity. For the limb IMUs, the corresponding ranges were 16 g for the low-g acceleration, 200 g for the high-g acceleration, and 2 000 degrees/s for the angular velocity. A sampling rate of 200 Hz was used for all IMUs, which were synchronised in time with < 100 ns accuracy (Bosch et al., 2018). Before every measurement, the accelerometers and gyroscope were calibrated during a 5-second period of signal silence, during which the cow was standing still. Here, acceleration (which should, under such circumstances, only be influenced by the gravity vector) and angular velocity were measured and the average offset was subtracted from the entire measurement (Bosch et al., 2018). The IMU data collected during measurements were transmitted wirelessly to the Inertia Gateway (Inertia Technology n.d.) plugged into a laptop computer running the Inertia Studio software (version 3.5.2).

During the measurements, one cow at a time was driven along the measurement aisle by one or two researchers, who interfered minimally with the cow to ensure as "natural" walking as possible. The cow walked up and down the measurement aisle one or two times, depending on the motivation of each cow. All measurements were filmed from the side using a handheld video camera (Canon Legria HF R78, Canon, Tokyo, Japan). One baseline measurement was performed for each cow, directly followed by at least two measurements where a mild to moderate grade of hindlimb lameness was induced (defined as degree 1–2 on a modified Sprecher scale ranging from 0 to 4 (Sprecher et al., 1997; Coetzee et al., 2014)). Induction measurements where the lameness did not remain stable (i.e. decreased or disappeared, as visually judged by $\geq$ 2 experienced assessors, who observed the cow during the entire measurement) were considered unsuccessful and discarded. After each induction measurement, the state of the induction device (see section "Lameness induction") was controlled in a trimming chute. If it was dispositioned or not intact, the measurement was discarded. In addition, the claw in question was inspected. The goal was to obtain 2 induction measurements per cow; if an induction measurement was deemed unsuccessful, a new attempt was made (within reasonable limits depending on each cow's motivation, which was judged individually). Each cow was assessed while walking postinduction to rule out persisting lameness. After data collection, video recordings of all measurements were, for descriptive purposes, graded by veterinarians using a modified version of the Sprecher scale (Sprecher et al., 1997; Coetzee et al., 2014), where score 0 (lowest) indicates no lameness, and score 4 (highest) indicates severe lameness (Coetzee et al. 2014). For an overview of all performed measurements, see Table 1. In connection with the experimental procedures described here, forelimb lameness was also induced in the cows (with separate baseline measurements performed for each cow before a session of forelimb induction measurements). Forelimb induction measurements and their corresponding baseline measurements constitute a separate experiment and associated dataset, which will be described elsewhere. Data from all baseline measurements are described in detail in Tijssen et al. (2021).

Lameness induction

Two principally different methods, intended to cause a reversible, mild to moderate degree of lameness, were employed. Before lameness induction, the cow was put in a trimming chute, where the claw which was subject to induction (left hind: N = 8, right hind: N = 9) was inspected. Then, lameness was induced using one of the following methods. In the first method, increased pressure was applied to the sole distal to the attachment site of the deep digital flexor tendon of the pedal bone of the lateral hind claw. The superficial layer of the sole horn of the weight−bearing surface of the lateral claw was first trimmed to allow for closer inspection, where continued absence of severe lesions was confirmed. Then, a wooden cylinder (height: 5–14 mm, adjusted as needed during experiment to achieve desired lameness degree, diameter: 10 mm) or a hollow, spherical plastic nut protection cap (Stabilit M6/M8 5552006/5552007, BAHAG AG, Germany), filled with chemical metal and further referred to as "plastic cap" (height: 5–15 mm, adjusted as needed during experiment to achieve wanted lameness degree) (Plastic Padding, Pattex, Sweden)

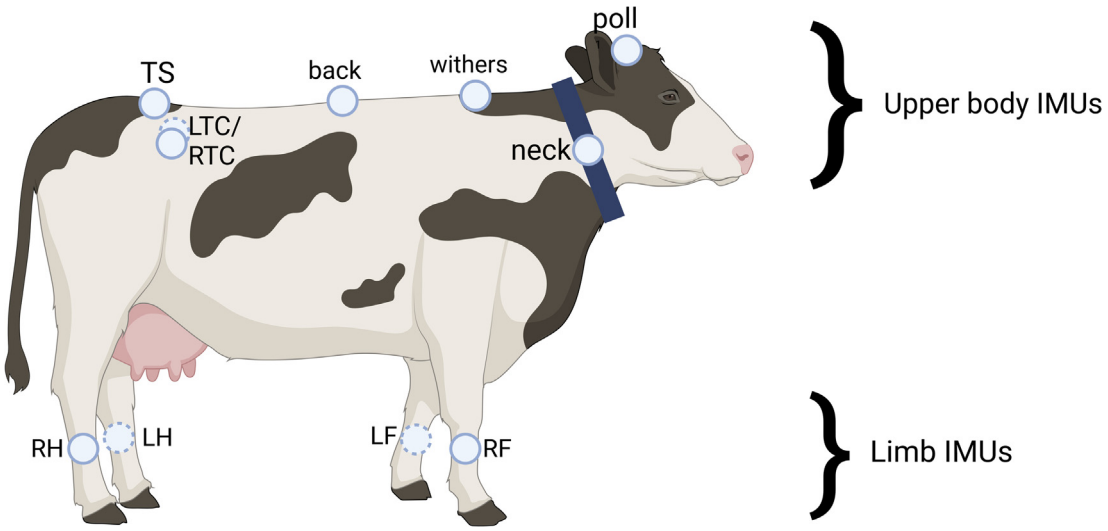

Fig. 1. Schematic figure showing the placements of inertial measurement units (IMUs) on the cow's body. Each IMU is represented by a white circle; a dashed circle contour indicates that the IMU is not visible from the right. The RH, LH, RF and LF IMUs are referred to as limb IMUs, and the remaining IMUs are referred to as upper body IMUs. TS=*tubera sacrale*, RTC=right *tuber coxae*, LTC=left *tuber coxae*, RH=right hind, LH=left hind, RF=right front, LF=left front. Figure created with BioRender.com.

Table 1
Overview of measurements performed for each cow. For included measurements, lameness grades (0–4) assigned during retrospective video assessment are given. Type of induction device (wooden cylinder/plastic cap/rubber block) is stated for all induction measurements. For the wooden cylinder, the diameter was always 10 mm; the size indication refers to the height of the device, which was adjusted as needed to obtain the desired degree of lameness. For the plastic cap, the size indication refers to the height of the device, which was adjusted as needed for each individual to obtain the desired degree of lameness. Italic font indicates that the measurement in question was discarded, either because of mechanical damage/loss of the induction device or because of non-visible/unstable lameness, as detailed in the footnotes. Abbreviations: LH=left hind, RH=right hind.

		Measurements overview				
		Baseline	Induction			
Cow	Induced limb	Lameness degree	Lameness degree/induction device	Lameness degree/induction device	Lameness degree/induction device	Lameness degree/induction device
1	LH	0	1/plastic cap 10 mm	2/plastic cap 15 mm	–	–
2	LH	2	–/plastic cap 10 mm[1]	3/plastic cap 15 mm	–	–
3	LH	0	–/plastic cap 10 mm[2]	–/plastic cap 15 mm[2]	–	–
4	LH	0	1/plastic cap 10 mm	1/plastic cap 15 mm	–	–
5	RH	0	–/plastic cap 10 mm[1]	3/plastic cap 15 mm	–/plastic cap 10 mm[2]	–
6	RH	0	1/plastic cap 10 mm	1/plastic cap 15 mm	–	–
7	LH	0	1/wooden cylinder 5 mm	–/wooden cylinder 11 mm[1]	–/wooden cylinder 11 mm[1]	
8	RH	0	1/plastic cap 10 mm	–/plastic cap 10 mm[2]	–	–
9	LH	0	2/plastic cap 10 mm	1/plastic cap 8 mm	–	–
10	RH	0	1/plastic cap 10 mm	1/plastic cap 15 mm	–	–
11	RH	0	1/plastic cap 10 mm	1/plastic cap 15 mm	–/rubber block 5 cm[2]	–
12	LH	0	–/wooden cylinder 6 mm[2]	–/wooden cylinder 13 mm[1]	1/rubber block 5 cm	–/wooden cylinder 14 mm[1]
13	RH	0	–/plastic cap 10 mm[1]	–/plastic cap 15 mm[2]	2/plastic cap 15 mm	–
14	RH	0	1/wooden cylinder 6 mm	2/wooden cylinder 10 mm	–	–
15	RH	0	–/plastic cap 10 mm[2]	2/plastic cap 10 mm	–	–
16	RH	0	2/plastic cap 10 mm	1/plastic cap 5 mm	–	–
17	LH	0	3/plastic cap 10 mm	1/wooden cylinder 6 mm	–	–

[1] Measurement excluded due to mechanical damage or loss of induction device.
[2] Measurement excluded due to non-visible or unstable lameness.

was attached to this location using cyanoacrylate glue (36–2375, Biltema, Sweden). Using hoof glue (Equi-Thane Superfast 47140, Vettec, The Netherlands or Bovi-Bond 46120, Vettec, The Netherlands), a ridge was created around the plastic cap or wooden cylinder to increase the attachment area. The plastic cap was prepared before experimental procedures; the cap was filled with the chemical metal solution and left to solidify overnight according to manufacturers' instructions. Thereby, a hard device capable of withstanding strong forces was created. After attachment of the induction device, the claw was wrapped in adhesive bandage, secured with adhesive tape as needed.

In the second method, increased pressure was applied to the interdigital space by using a rubber block, 17 mm thick and 50 mm high, exceeding the height of the claws so the block protruded about 20–30 mm beneath the sole. The block was secured with elastic bandage and adhesive tape as needed. To avoid wounds, a plastic film was placed between the rubber block and the skin to reduce friction. Lameness induction procedures are visualised and explained in a step-by-step manner in Fig. 2.

Data processing

Initial processing and data selection

The raw IMU data (i.e. accelerometer and gyroscope data) were exported to MATLAB (version R2023a, the MathWorks Inc, Natick, United States) and analysed using scripts originally developed for

Fig. 2. Lameness induction procedure, explained and visualised in a step-by-step fashion. The upper images, inside the orange square, depict the sole pressure approach: either a plastic nut protection cap filled with metal (2a) or a wooden cylinder (2b) was used. When the plastic nut protection cap was used, this was filled with liquid, chemical metal which was left to harden according to the manufacturer's instructions prior to experimental procedures. Image (1) shows a plastic nut protection cap before filling with metal. Prior to lameness induction, the cow was fixated in a trimming chute. The superficial layer of the sole horn of the claw which was to be induced was trimmed (3). The induction device (wooden cylinder or plastic cap) was then glued to the caudal third of the sole of the lateral hind claw; 4a, 4b) using cyanoacrylate glue. A ridge of hoof glue was created around the device to increase the attachment area (5). The device was secured with elastic bandage and adhesive tape (6). The lower images, inside the purple square, depict the interdigital pressure approach: a rubber block (1) was used to create pressure in the interdigital space. The cow was fixated in a trimming chute, and the rubber block was placed in the interdigital space such that 2–3 cm of the block protruded beneath the sole (2). A plastic film was placed between the block and the skin to avoid bruising. The block was tied in place using elastic bandage (3), and then secured with elastic bandage and adhesive tape (4).

horses. Angular velocity was integrated to obtain orientation for each IMU as described in Valenti et al. (2015). Based on the determined orientation, the acceleration measured by each IMU was rotated from a local to a global reference frame, where the Z-axis was aligned with gravity (the X and Y axes were set arbitrarily since their positive directions were not meaningful for the current study) (Bosch et al., 2018). Foot-on and foot-off timings were calculated using algorithms originally developed for horses (Serra Bragança et al., 2017). Data were selected as described in Tijssen et al. (2021) using generated plots showing the stance phases of each claw relative to time, and synced with video recordings. Up to four segments of data per measurement were selected for analysis. A segment was included if the cow was walking in a straight line (i.e. no halts or turns) with no to minimal physical handling, and if the footfall plot indicated a four-beat walking pattern (Fig. 3).

Calculation of upper body kinematic parameters

The goal of this part of data processing was to describe pelvic rotation and upper body vertical displacement, including vertical range of motion (**ROMz**) and within-stride vertical displacement asymmetry of the upper body midline. At the walk, the highest vertical position of the withers and sacrum is normally seen around mid-stance of the fore- and hindlimb, respectively, while the lowest vertical position is seen around maximal spread (i.e. when one limb is protracted and the other one retracted) of the fore- and hindlimbs, respectively (Serra Bragança et al., 2021; Tijssen et al., 2021; Smit et al., 2023). The head-and-neck-segment oscillates with a phase shift compared to the withers such that energy consumption is minimised (Loscher et al., 2016). Thus, vertical displacement of the upper body midline during one stride cycle theoretically takes the shape of a sinusoid-like curve with two periods. Vertical asymmetry can therefore be quantified by calcu-

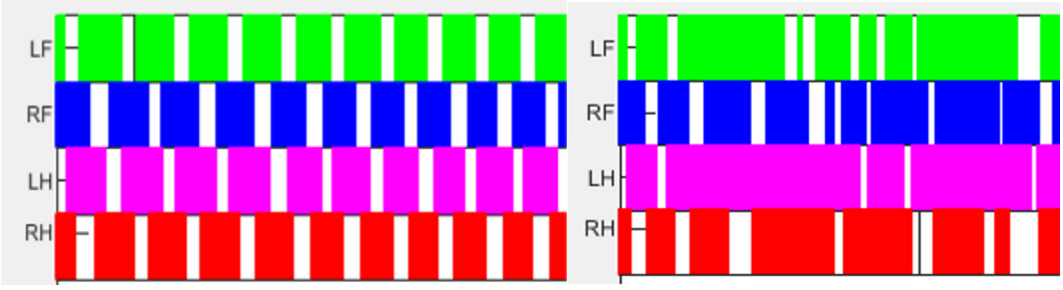

Fig. 3. Snippets from generated footfall plots, which were used together with video recordings of the cows from the measurements, to select segments for analysis. Green: left front stance (LF), blue: right front stance (RF), pink: left hind stance (LH), red: right hind stance (RH). Left: example from footfall plot, showing part of segment which was selected for analysis, indicating regular four-beat walking pattern. Right: example from footfall plot, showing segment which was not selected for analysis as the footfall pattern does not indicate walk.

lating within-stride differences in the vertical displacement's local maxima and minima, respectively. Increased differences imply that within-stride vertical asymmetry is increased. Another way to quantify within-stride vertical asymmetry is to extract the main frequency components (i.e. harmonics of the stride frequency) from the vertical displacement signal. Harmonics are essentially sine waves; the first harmonic oscillates with the stride frequency, the second harmonic oscillates with 2x the stride frequency, etc. Due to the nature of these gaits, it is assumed that the vertical displacement signals of the upper body midline can largely be reconstructed from the first and second harmonic. When within-stride vertical asymmetry increases, the first harmonic's amplitude increases relative to the second harmonic's amplitude (Peham and Scheidl, 1996; Keegan et al., 2001; Audigié et al., 2002). See Fig. 4 for an illustration of this concept. In the current study, both aforementioned approaches were applied, although the former one was only used for the withers and TS IMUs. This decision was made because this method requires that the signal contains two relatively clear maxima and minima per stride, which can be expected from the withers and TS IMUs. The remaining upper body IMUs are expected to produce signals where e.g. smaller "peaks" additional to the underlying sinusoid pattern are common, making correct detection of maxima and minima problematic (Tijssen et al., 2021).

Vertical displacement was, as in Tijssen et al. (2021), calculated from the acceleration measured by the upper body IMUs following adjustment for IMU orientation (rotating the measured accelerations to align with gravity). This was done using a cyclic double integration algorithm described by Pfau et al. (2005). To obtain correct calculations, high- and low-frequency noise, caused by e.g. shaking of IMUs and erratic head movements, needed to be removed from the signal. The vertical displacement signal was therefore high-pass filtered using a cut−off frequency of 0.2 Hz, and low-pass filtered using a cut−off frequency of 10 × stride frequency (for our data, mean stride duration was 1.33 s with a SD of 0.162, translating to an average stride frequency of 0.75 strides/second). The signal was then split into strides based on the timing of the foot-on of the left hindlimb (Bosch et al., 2018). Next, the desired upper body parameters could be calculated. Vertical range of motion (ROMz) was calculated, for each stride, as the difference between the minimum and maximum value of the vertical displacement signal for the poll, neck, withers, back and TS IMUs, respectively. The within-stride differences between the two maximum/minimum positions of the withers/TS IMUs (withers_Maxdiff, withers_Mindiff, TS_Maxdiff, and TS_Mindiff) were calculated as follows (also visualised in Fig. 5). Withers_Maxdiff/TS_Maxdiff: the local vertical maximum associated with the RF/RH mid-stance phase was subtracted from the one associated with the LF/LH mid-stance phase. Withers_Mindiff: the local minimum associated with the protraction of LF and retraction of RF was subtracted from the one associated with the opposite situation, i.e. protraction of RF and retraction of LF. TS_Mindiff: the local minimum associated with the protraction of RH and retraction of LH was subtracted from the one associated with the opposite situation, i.e. protraction of LH and retraction of RH. For example, a negative TS_Mindiff hence stipulates that the TS reached a lower position during early stance phase of LH compared to early stance phase of RH; a positive TS_Mindiff stipulates the opposite (i.e. lower TS position during early stance of RH compared to LH). Then, the first two main frequency components, or harmonics, of the poll, neck, withers, back and TS IMUs' vertical displacement were extracted using a signal decomposition method described in detail in Roepstorff et al. (2021), for each IMU and stride separately. In this process, the vertical displacement signal (for each IMU and stride) was replicated ≥ 3 times and concatenated to obtain a periodic signal, thereby enabling Fourier analysis of a single stride. Then, the vertical displacement signal of each stride was subjected to fast Fourier transform, and the amplitudes of the first and second harmonic waves (z_h1_amp and z_h2_amp) of the IMUs in question were computed and expressed as a ratio between 0 and 1 of the total range of motion (Roepstorff et al., 2021).

To quantify pelvic rotation, roll and pitch angles were calculated. Pitch angle was obtained from the determined orientation of the TS IMU. Range of motion (i.e. the difference between the maximum and minimum value) of the pitch angle (TS_pitch) was

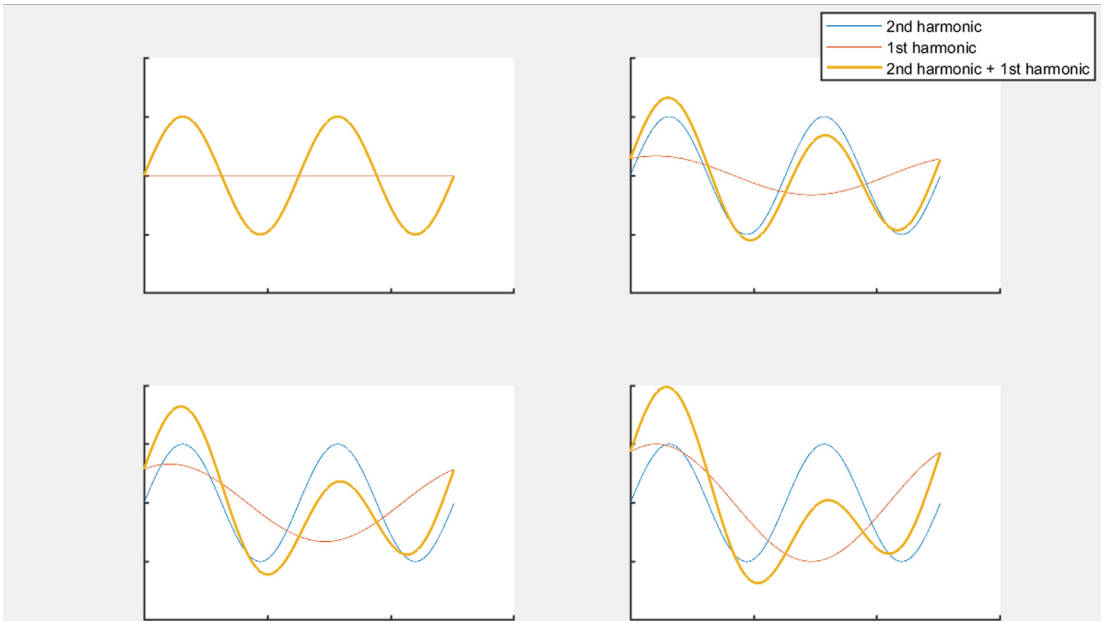

Fig. 4. Schematic, Matlab-generated representation, intended to illustrate upper body vertical displacement in a cow during one stride cycle, as well as the effects of an increased first harmonic amplitude relative to the second harmonic amplitude. The signal contains two peaks and two valleys, and is reconstructed by its first (red line) and second (blue line) harmonics. A: the amplitude of first harmonic = 0 (represented by flat line), i.e. second harmonic is identical to reconstructed signal (yellow, line), which is completely bilaterally symmetrical. In the following plots (B, C, D), the first harmonic amplitude (i.e. the asymmetric component) is increased while the second harmonic (i.e. the symmetric component) amplitude is kept constant, resulting in an increasingly asymmetric resulting curve.

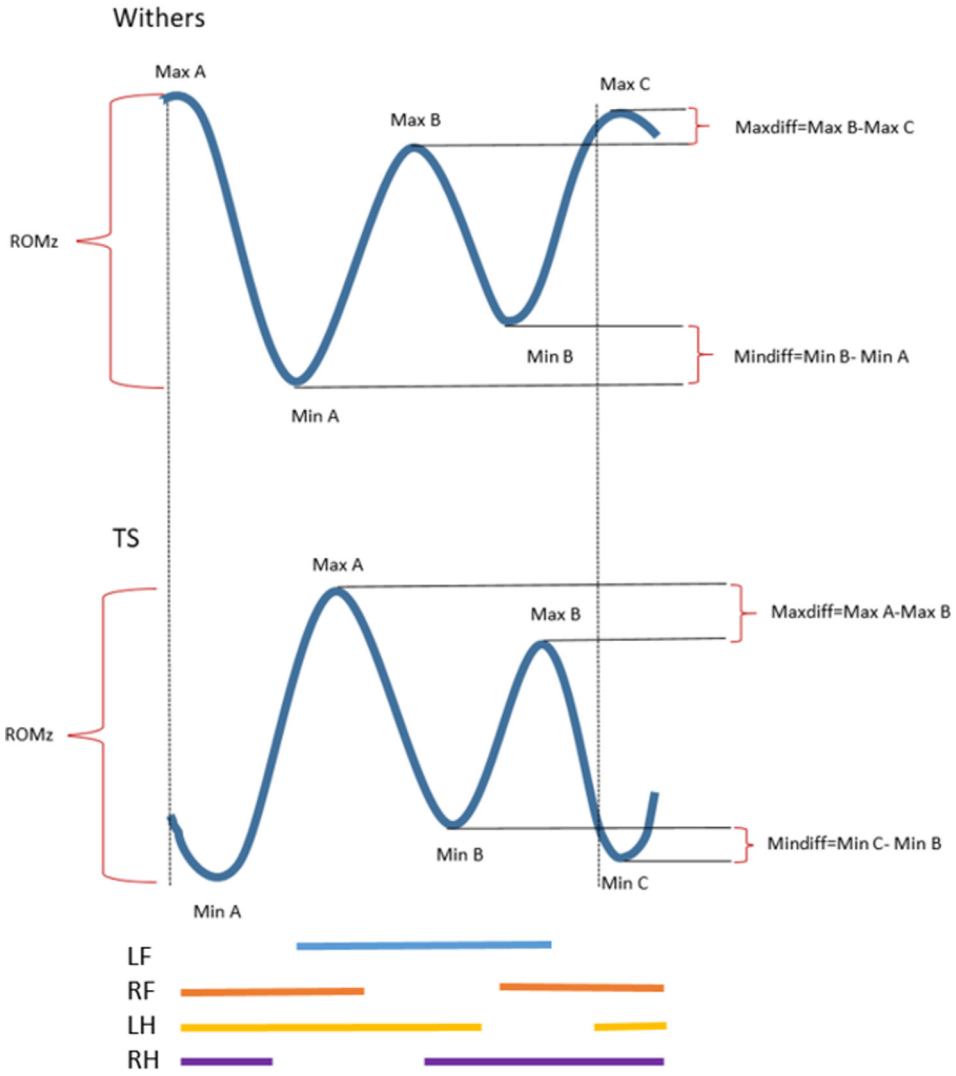

Fig. 5. Simulated representation illustrating an example of vertical displacement of withers and *tubera sacrale* (TS), respectively, starting at foot-on of left hindlimb (indicated by dashed line). Footfalls are indicated in bottom; RF=right front, LF=left front, RH=right hind, LH=left hind. Maxdiff is defined as the within-stride difference between the two local maxima, and Mindiff is defined as the within-stride difference between the two local minima. Withers_Maxdiff, Withers_Mindiff, TS_Maxdiff, and TS_Mindiff are caculated as indicated in the figure. Hence, a negative withers_Maxdiff stipulates that the cows' withers reached a higher position during mid-stance of RF compared to mid−stance of LF; a positive withers_Maxdiff stipulates the opposite (i.e. a higher position during mid-stance of LF compared to RF). A negative withers_Mindiff stipulates that the withers reached a lower position during early stance of RF compared to early stance of LF; a positive withers_Mindiff stipulates the opposite. A negative TS_Maxdiff stipulates that the TS reached a higher position during mid−stance of RH compared to mid−stance of LH; a positive TS_Maxdiff stipulates the opposite. A negative TS_Mindiff stipulates that the TS reached a lower position during early stance of LH compared to early stance of RH; a positive TS_Mindiff stipulates the opposite. ROMz = maximum vertical range of motion during one stride cycle.

then calculated for each stride. Roll angle was instead calculated from the vertical displacement of the RTC and LTC IMUs, assuming a pelvic width of 55 cm. The rotation was centred on zero over time. This was deemed more appropriate than obtaining this measure from the orientation of the TS IMU, as its rolling pattern is likely to be disturbed by the IMU rolling from side to side over the spinous processes as the cow is walking. This approach enables detection of asymmetry between the left and right steps, as well as overall range of motion, but not "static offset", i.e. consistent drop of one hip. Range of motion of the roll angle (pelvis_roll) was, as for pitch, calculated for each stride. Then, the first and second harmonics' relative amplitudes (pelvis_roll_h1_amp and pelvis_roll_h2_amp) of the roll angle were extracted for each stride using the same method as for the vertical displacement signals (Roepstorff et al., 2021). For visualisation of pitch and roll and definition of positive and negative directions of rotation, see Fig. 6.

For visualisation purposes, vertical displacement for the poll, neck, withers, back and TS IMUs was plotted for each measurement, similarly as described in (Tijssen et al., 2021). The vertical displacement signal of each stride was plotted as a separate line, and time normalised (i.e. depicted on a scale from zero to 100) so that all strides start at 0% (LH foot-on) and end at 100% (subsequent LH foot-on) (Tijssen et al., 2021). Most common stride (defined as the stride differing the least from the remaining ones) was calculated for each measurement and depicted in the figures. Mean footfall timings for every limb were plotted accordingly to visualise stance phases. Pitch and roll angle curves were plotted similarly, but without indication of footfall timings and most common stride.

Calculation of limb kinematic parameters

The goal of this part of data processing was to obtain both spatial and temporal parameters related to the limb motion. Stride duration was calculated as the time between two consecutive LH foot-on moments. As in Tijssen et al. (2021), maximum protraction and retraction angles (re_max and pro_max) of the metatarsal seg-

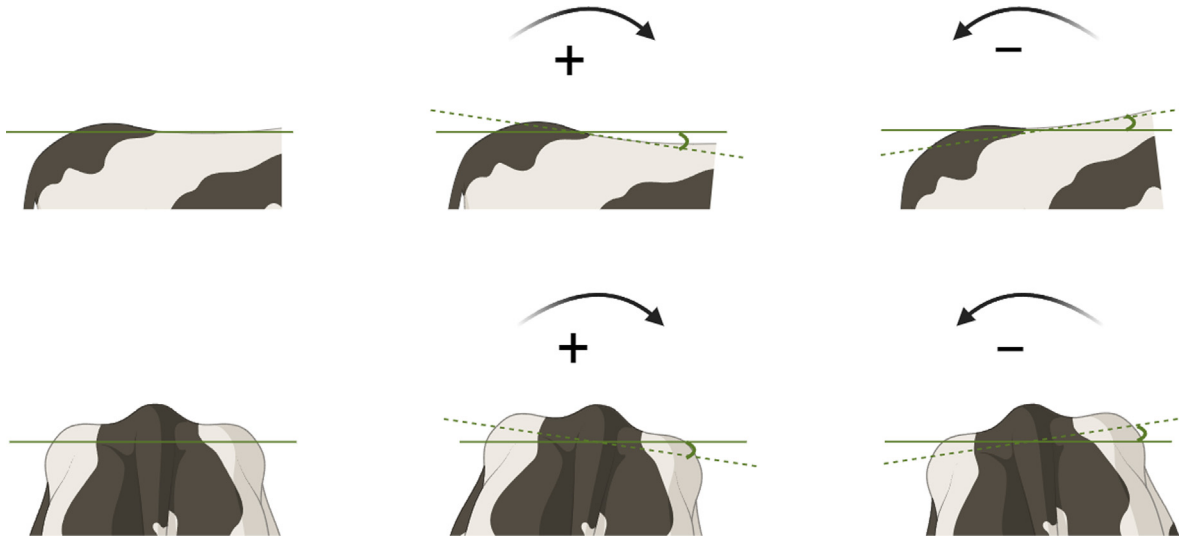

Fig. 6. Visualisation of roll and pitch of a cow's pelvis. Positive (+) and negative (−) directions are indicated by arrows. Top: visualisation of pelvic roll. Top left: neutral position. Top middle: rotation in direction defined as positive (clockwise rotation as seen from behind). Top right: Rotation in direction defined as negative (counter-clockwise rotation as seen from behind). Bottom: visualisation of pelvic pitch. Bottom left: neutral position. Bottom middle: rotation in direction defined as positive (clockwise rotation as seen from the right). Bottom right: Rotation in direction defined as negative (counter-clockwise rotation as seen from the right). Figure created with BioRender.com.

ment were calculated for each stride, from the sagittal orientation obtained for the LH and RH IMUs, as described in Bosch et al. (2018). Protraction (forward extension, seen in early stance phase/late swing phase) was set as positive direction, and retraction (backwards extension, seen in late stance phase/early swing phase) was set as negative direction. Thus, maximum protraction angle values are positive, and maximum retraction angles are negative. Furthermore, diagonal and lateral dissociation (diag_diss and lat_diss) were calculated for both sides in each stride. Diag_diss is defined as the time between foot-on of either forelimb and foot-on of the contralateral hindlimb, expressed as a ratio of the duration of the entire stride. Lat_diss is the time between foot-on of either hindlimb and foot-on of the ipsilateral forelimb, as a ratio of stride duration. As these measures are based on the sequential foot placement in the normal walking gait, the sum of the four temporal measures of one same stride always equals to 1, and the measures would make up 0.25 each of the stride duration in a theoretical, "perfectly uniform" walk where all four foot-on moments are equally spaced in time. For an overview of all calculated kinematic parameters and abbreviations, see Table 2.

Visual evaluation of data and validation of parameters

Data for all measurements were evaluated with regard to quality using stride-by-stride-plots displaying limb and upper body data. Since the goal was to detect data affected by obvious instrumentation errors, this was done visually (i.e. no automatic outlier removal procedure was applied). Protraction/retraction angle curves of all limb IMUs were plotted against time. When artefacts (stemming from raw gyroscope data and likely due to measuring errors) were visually seen in the angle curve associated with the LF and/or RF IMU, temporal parameters (diag_diss and lat_diss) of associated strides (n = 29) were excluded. When artefacts were caused by the RH IMU, maximal protraction and retraction angles (re_max and pro_max) and temporal parameters of associated strides (n = 104) were excluded. When disturbances were seen in the angle curve associated with the LH IMU, all data associated with those strides (n = 161) were excluded as the LH IMU was used for stride segmentation; errors from this IMU could affect the calculation of all parameters. The vertical displacement of the withers and TS IMUs were plotted against time and evaluated visually. Automatically identified local maxima and minima were displayed. Due to incorrect identification, Maxdiff and Mindiff values were excluded from 26 and 25 strides, respectively, for the withers IMU and from three and 11 strides, respectively, for the TS IMU. Due to visually detected registration errors, data from the TS IMU were excluded from a further 61 strides for one cow (cow 17). For further explanations and visualisation of these procedures, see Supplementary Figure S1, and for an overview of included data, see Supplementary Table S1.

Statistical analysis of data

Statistical analysis was conducted in R version 4.2.1 (R core team, 2023), in the environment RStudio version 2023.06.0 (Posit team, 2023). Analyses were performed on stride-by-stride data. As some of our parameters compare the motion between the left and right steps, these data needed to be "mirrored" to prevent values from cows with lameness in different limbs to "cancel out" each other. Prior to statistical analysis, all Maxdiff and Mindiff values (both from baseline and induction measurements) were therefore multiplied by −1 for cows with a left hindlimb induction. Maximum protraction and retraction angles were switched between the left and right limb (in baseline as well as in induction measurements) for cows with a left hindlimb induction. Diag_diss and lat_diss values were switched in a similar fashion pertaining to the involved hindlimb; for example, all lat_diss data involving the right hindlimb were switched with lat_diss data involving the left hindlimb, in cows with a left hindlimb induction. Data from cows with a right hindlimb induction were left unaltered. The left hindlimb was labelled "non-induced limb", and the right hindlimb was labelled "induced limb" in all instances. Hence, in the statistical analyses, all cows were treated as if lameness had been induced in the right hindlimb, and comparisons between the baseline and induction conditions could be made without taking the side of the induction into account. If <15 strides/measurement were available for analysis of a parameter, the parameter was not included in statistical analysis for the measurement in question. This criterion was applied based on recommendations from the manufacturer of the IMU system and led to the exclusion of withers_Maxdiff and withers_Mindiff data for one cow (cow 2).

Table 2
Kinematic parameters which were, for each cow and measurement, calculated on a stride-by-stride basis for the selected segments of data.

Explanation of kinematic parameters	
Parameter	Explanation
re_max (induced/non-induced limb)	Maximum retraction angle in degrees, calculated for both hindlimbs
pro_max (induced/non-induced limb)	Maximum protraction angle in degrees, calculated for both hindlimbs
diag_diss (induced/non-induced limb involvement)	Time between foot-on of forelimb and following contralateral hindlimb as ratio of stride duration, calculated for both sides
lat_diss (induced/non-induced limb involvement)	Time between foot-on of hindlimb and following ipsilateral forelimb as ratio of stride duration, calculated for both sides
withers_Maxdiff	Within-stride difference between local maxima for the withers in millimetres
withers_Mindiff	Within-stride difference between local minima for the withers in millimetres
TS_Maxdiff	Within-stride difference between local maxima for the *tubera sacrale* in millimetres
TS_Mindiff	Within-stride difference between local minima for the *tubera sacrale* in millimetres
poll_ROMz	Vertical range of motion of the poll in millimetres
neck_ROMz	Vertical range of motion of the neck in millimetres
withers_ROMz	Vertical range of motion of the withers in millimetres
back_ROMz	Vertical range of motion of the back in millimetres
TS_ROMz	Vertical range of motion of the *tubera sacrale* in millimetres
poll_z_h1_amp	Amplitude[1] of the first harmonic for vertical displacement of the poll
poll_z_h2_amp	Amplitude[1] of the second harmonic for vertical displacement of the poll
neck_z_h1_amp	Amplitude[1] of the first harmonic for vertical displacement of the neck
neck_z_h2_amp	Amplitude[1]of the second harmonic for vertical displacement of the neck
withers_z_h1_amp	Amplitude[1] of the first harmonic for vertical displacement of the withers
withers_z_h2_amp	Amplitude[1] of the second harmonic for vertical displacement of the withers
back_z_h1_amp	Amplitude[1] of the first harmonic for vertical displacement of the back
back_z_h2_amp	Amplitude[1] of the second harmonic for vertical displacement of the back
TS_z_h1_amp	Amplitude[1] of the first harmonic for vertical displacement of the *tubera sacrale*
TS_z_h2_amp	Amplitude[1] of the second harmonic for vertical displacement of the *tubera sacrale*
pelvis_roll	Range of motion of pelvic roll angle in degrees
pelvis_roll_h1_amp	Amplitude[1] of the first harmonic of pelvic roll angle
pelvis_roll_h2_amp	Amplitude[1] of the first harmonic of pelvic roll angle
TS_pitch	Range of motion of pitch angle of the *tubera sacrale* in degrees

[1] Expressed as a ratio between 0 and 1 of the total range of motion.

Baseline and induction measurements were compared in linear mixed models using the function "lmer" from the package "lme4" (Batens et al., 2015). One model was created for each of the continuous outcome parameters summarised in Table 2. In all models, "condition" (i.e. baseline or induction) was set as fixed factor. As the subjects contributed with unequal numbers of measurements and strides within measurement, "cow" and "measurement within individual" were set as random effects in all models. Stride duration in seconds (as proxy for speed; an increase in stride duration corresponds to a decrease in speed) was included as a linear fixed factor in all models. This was done to improve model fit as speed is known to influence kinematic gait parameters (Walker et al., 2010; Weishaupt et al., 2010). The effect of condition on stride duration was tested in a separate model with stride duration as outcome parameter, condition as fixed factor, and cow as well as measurement as random effects. Furthermore, the interaction between stride duration and condition was tested in all models. The interaction was kept in models where it was statistically significant (as judged from F-tests, see below). Stride duration was kept as a linear fixed factor in all models, whether significant or not.

Type III ANOVAS (package:"car" (Fox and Weisberg, 2019)) with Kenward-Roger degrees of freedom (package: "pbkrtest" (Halekoh and Højsgaard, 2014)) were computed, and Wald F-tests were calculated. Using grand mean stride duration, estimated marginal means for the two conditions, as well as *P*-values for the difference between the two conditions, were calculated using the "emmeans" function from the package "emmeans" (Lenth, 2023). Slope estimates were, for all models, calculated for the two conditions using the "emtrends" function, also from the package "emmeans" (Lenth, 2023). Normality and homoscedasticity of residuals were visually assessed using quantile–quantile plots and residual plots (Kozak and Piepho, 2017). Significance level was set to < 0.05 for all analyses.

Results

A total of 41 measurements, where 16 cows contributed with one baseline measurement and one or two induction measurements each, were included in analyses. Fifteen measurements were discarded due to failure in inducing lameness (defined as substantial mechanical damage to the induction device and/or unstable lameness, as judged visually). Thus, of the 17 initially included cows, one (cow 3) was completely excluded from analyses due to failure in successfully inducing a stable lameness in any of the attempts made. In all other measurements, lameness induction thus resulted in a gait which was visually identical to that seen in "natural" lameness; however, none of the cows showed any signs of residual lameness after removal of the induction device. Apart from a small indentation mark in the claw horn of one of the cows (cow 1), no visible lesions were found following lameness induction in any of the animals. See Table 1 for an overview of all measurements. Moreover, 3 475 strides were initially selected for analysis. After exclusions following visual evaluation, data from a total of 3 314 strides were finally included in statistical analyses, ranging between 15 and 132 strides/measurement. For full details about included strides per measurement and parameter, as well as reasons for exclusion, see Supplementary Table S1.

Linear mixed model analysis

For poll_ROMz, neck_ROMz, back_ROMz, and TS_ROMz, the outcome variable was log−transformed (natural logarithm), and for TS_z_h1_amp as well as pelvis_roll_h2_amp, it was square-root transformed due to heteroscedasticity and non-normality of residuals. For all the remaining parameters, the residuals were approximately normally distributed, and no severe signs of heteroscedasticity were seen. Thus, for the statistical models con-

Table 3
Results from linear mixed model analysis following computation of kinematic parameters for each stride and measurement (N=16 cows). Estimated marginal means and *P*-values for differences between baseline and induction condition (computed at grand mean stride duration) and corresponding estimated regression slope parameters. A slope estimate of 1 indicates that a 1−second increase in stride duration corresponds to a 1−unit increase in the outcome parameter. Identical slopes for baseline and induction condition indicate that no interaction term was included, i.e. stride duration was assumed to have the same effect on the outcome parameter irrespective of condition. For outcome variables that were transformed prior to analysis, estimates are given on the transformed scale. Abbreviations are defined in Table 2.

Linear mixed model analysis results						
Outcome variable	Model estimate[1]; baseline	Model estimate[1]; induction	Contrast *P*-value	Slope estimate; baseline	Slope estimate; induction	RSD
re_max (non-induced limb)	−29.50	−28.60	0.024	6.01	3.55	2.08
pro_max (non-induced limb)	24.00	23.70	0.29	−2.58	−2.58	1.74
re_max (induced limb)	−29.30	−30.00	0.40	6.06	6.06	2.47
pro_max (induced limb)	24.00	22.60	0.011	−2.77	−1.12	1.90
diag_diss (induced limb involvement)	0.259	0.279	0.0096	0.021	0.053	0.036
diag_diss (non-induced limb involvement)	0.251	0.229	0.0083	0.024	−0.0062	0.030
lat_diss (induced limb involvement)	0.241	0.254	0.15	−0.014	−0.014	0.035
lat_diss (non-induced limb involvement)	0.249	0.238	0.045	−0.032	−0.032	0.031
withers_maxdiff	−0.22	4.53	0.0033	−0.96	−7.99	7.15
withers_mindiff	−5.40	−4.64	0.81	−1.05	6.53	8.53
TS_maxdiff	−0.13	−0.12	0.99	1.43	1.43	6.22
TS_mindiff	−0.23	−4.84	0.033	−1.80	−8.85	8.34
poll_ROMz	4.19	4.55	0.0024	0.57	0.21	0.41
neck_ROMz	4.03	4.34	0.0079	0.74	0.45	0.39
withers_ROMz	39.9	45.5	<0.001	−9.50	−9.50	6.66
back_ROMz	3.09	3.29	0.016	0.20	0.20	0.23
TS_ROMz	3.66	3.74	0.062	−0.40	−0.29	0.17
poll_z_h1_amp	0.42	0.52	0.0018	0.16	0.029	0.14
poll_z_h2_amp	0.37	0.31	0.014	−0.33	−0.19	0.12
neck_z_h1_amp	0.40	0.48	0.0030	0.033	−0.061	0.13
neck_z_h2_amp	0.32	0.28	0.021	−0.12	0.0017	0.10
withers_z_h1_amp	0.22	0.24	0.032	0.16	0.026	0.074
withers_z_h2_amp	0.50	0.47	0.012	−0.27	−0.19	0.064
back_z_h1_amp	0.25	0.35	<0.001	0.13	−0.023	0.089
back_z_h2_amp	0.41	0.31	<0.001	−0.18	−0.085	0.077
TS_z_h1_amp	0.41	0.46	0.0098	0.19	0.083	0.10
TS_z_h2_amp	0.63	0.57	0.0035	−0.40	−0.23	0.086
pelvis_roll	8.04	8.23	0.38	−1.11	0.14	1.22
pelvis_roll_h1_amp	0.65	0.58	0.0012	−0.21	−0.10	0.055
pelvis_roll_h2_amp	0.24	0.31	<0.001	0.085	−0.056	0.066
TS_pitch	6.96	7.59	0.053	0.56	1.51	1.08

[1] Estimated marginal mean.

cerning these parameters, original data were used. The linear mixed model analyses showed significant differences between baseline and induction measurements (at grand mean stride duration) in 23 out of 31 models. Estimated marginal means (calculated for grand mean stride duration), SEs, and contrast *P*-values for differences between baseline and induction measurements are summarised in Table 3 along with regression slope estimates.

Hence, lameness induction resulted in kinematic changes in multiple anatomical locations. In short, foot-on of the lame limb was (relatively seen) delayed, and the metatarsal segment of the lame limb was less protracted compared to the baseline condition. Foot-on of the non-induced hindlimb, and the forelimb contralateral to the induced limb, both occurred (relatively seen) earlier in the induction condition compared to the baseline condition. Furthermore, there were increased between stride-half differences in the vertical displacement of the poll, neck, withers, back and TS. For the withers and TS, the increased degree of vertical asymmetry seemed associated with early stance of the induced hindlimb. There were also changes in the main components of pelvic roll. In the following sections, the results are described in detail.

Limb kinematic parameters

Among the distal limb angles, significant decreases for re_max of the non-induced limb (1.1 degrees absolute difference) and pro_max of the induced limb (1.4 degrees absolute difference) were seen in the induction condition as compared to the baseline condition. No significant changes in re_max (induced limb) or pro_max (non-induced limb) were detected. Diag_diss (induced limb involvement) increased by 0.020 (ratio of stride duration), which is interpreted as an increased time between the consecutive foot-ons of the forelimb diagonal to the induced hindlimb, and the induced hindlimb. Diag_diss (non-induced limb involvement) and lat_diss (non-induced limb involvement) both decreased significantly by 0.022 and 0.011 respectively, which translates to a decreased time between the foot-ons of the forelimb diagonal to the non-induced hindlimb and the non-induced hindlimb, and between the foot-ons of the non-induced hindlimb and its ipsilateral forelimb. No significant change in lat_diss (induced limb involvement) was detected (See Fig. 7).

Upper body kinematic parameters

For the withers and TS IMUs, significantly increased degrees of within-stride asymmetry which were temporally related to the early stance phase of the induced limb were seen. A significant difference between conditions was detected in withers_Maxdiff. In the induction condition, the difference between the two local maxima (seen during mid-stance of each forelimb) of the withers was increased by 4.31 mm on average. The withers_Maxdiff estimate for the induction condition is positive, indicating that a higher position was reached during mid-stance of the forelimb diagonal to the induced hindlimb, compared to the forelimb ipsilateral to the induced hindlimb. Mid−stance of the forelimb is temporally closely related with early stance phase of its diagonal hindlimb; in the induction condition, the withers hence reached a higher position during the early stance of the induced compared to the non-induced hindlimb. A significant difference was also detected

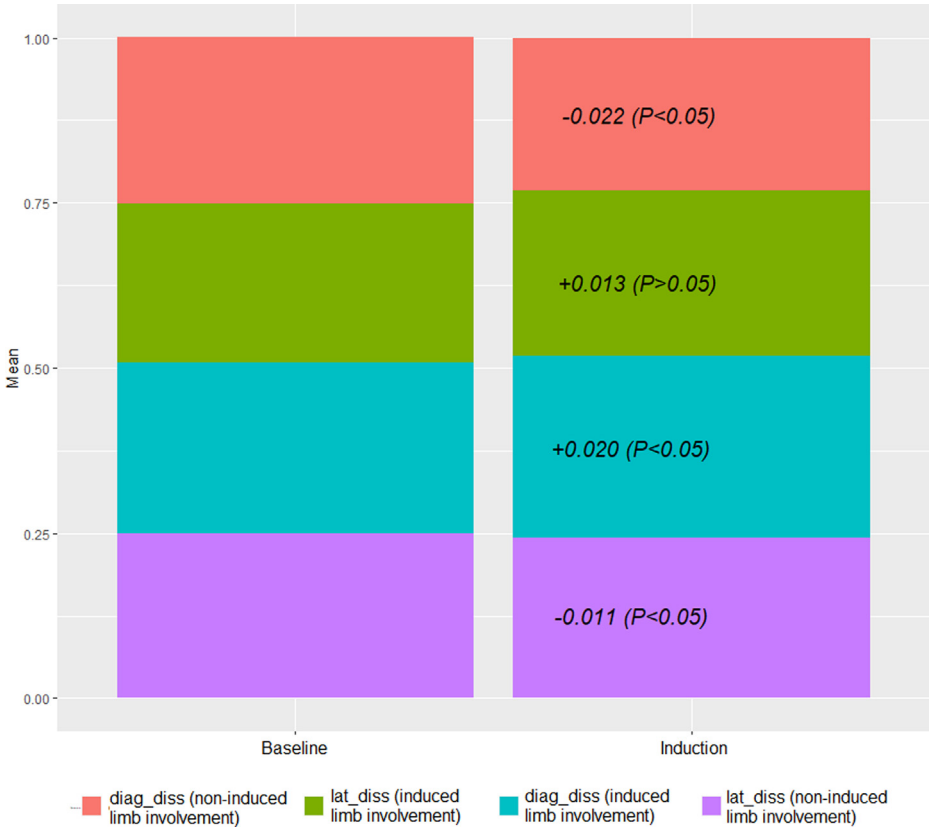

Fig. 7. Bar plots showing the average diag_diss (induced limb involvement) in pink, diag_diss (non-induced limb involvement) in green, lat_diss (induced limb involvement) in blue, and lat_diss (non-induced limb involvement) in purple, for the baseline and the induction condition respectively, with changes occurring with lameness induction indicated for each parameter. Values were, for both conditions, first averaged over each cow, and subsequently over each parameter. These parameters were calculated as a ratio of the total stride duration, i.e. their sum for each stride is always one. Significant decreases in diag_diss (non-induced limb involvement) and lat_diss (non-induced limb involvement) were detected, as well as a significant increase in diag_diss (induced limb involvement). Lat_diss (induced limb involvement) was not significantly altered by lameness induction.

for TS_mindiff. In the induction condition, the difference between the two minimum positions (seen during limb spread of the hindlimbs) of the TS IMU increased with 4.61 mm on average, where (as the TS_Mindiff estimate for the induction condition is negative) a higher position of the TS IMU was seen during early stance phase of the induced compared to the non-induced hindlimb. No significant changes in withers_Mindiff or TS_Maxdiff were detected.

Increased within-stride asymmetry in the vertical displacement of the midline of the upper body was further demonstrated by lameness-associated increases in the vertical displacements' first harmonic amplitude, and decreases in the vertical displacements' second harmonic amplitude, for the poll, neck, withers, back, and TS IMUs (all $P < 0.05$), (visualised in Fig. 8). These changes were most obvious for the poll and back IMUs; poll_z_h1_amp increased by 0.10, poll_z_h2_amp decreased by 0.06, back_z_h1_amp increased by 0.10, and back_z_h2_amp decreased by 0.10. The increased within-stride vertical asymmetry was coupled with significant increases in the ROMz per stride for the poll, neck, withers and back (all $P < 0.05$) IMUs. TS_ROMz was also increased, although not statistically significant ($P = 0.062$). Vertical displacement for all included measurements is visualised in Fig. 9 and Supplementary Figure S2.

Pelvis_roll was not significantly altered by induction of lameness. However, pelvis_roll_h1_amp decreased while pelvis roll_h1_amp increased (both $P < 0.05$, visualised in Fig. 10). Thus, as opposed to the situation for upper body vertical displacement, the relationship between the main components of the curve shape was altered without any changes in ROM. TS_pitch increased with lameness induction, but the change was not statistically significant ($P = 0.053$). Roll and pitch angle curves for all included measurements are visualised, and further explained, in Fig. 11 and Supplementary Figure S3.

Effect of stride duration

In the baseline condition, estimated marginal mean for stride duration was 1.33 s (95% confidence interval: 1.27–1.40), and in the induction condition, estimated marginal mean was 1.33 s (95% confidence interval: 1.27–1.39). Hence, there was no significant difference in stride duration between the two conditions ($P > 0.80$). Stride duration contributed significantly (all $P < 0.05$) in all models except for TS_Maxdiff, neck_Z_h1_amp, and pelvis_roll_h2_amp. The interaction between stride duration and condition was significant (all $P < 0.05$), and thus kept, in the models for the following outcome parameters: re_max (non-induced limb), pro_max (induced limb), diag_diss (non-induced limb involvement), diag_diss (induced limb involvement) withers_Maxdiff, withers_Mindiff, TS_mindiff, poll_ROMz, neck_ROMz, TS_ROMz, TS_pitch, pelvis_roll, poll_z_h1_amp, poll_z_h2_amp, neck_z_h1_amp, neck_z_h2_amp, withers_z_h1_amp, withers_z_h2_amp, back_z_h1_amp, back_z_h2_amp, TS_z_h1_amp, TS_z_h2_amp, pelvis_roll_h1_amp, and pelvis_roll_h2_amp. This implies that stride duration had different effects on these outcome parameters depending on the condition (baseline or induction), as indicated by the slope estimates presented in Table 3. For example, in the case of neck_z_h2_amp, increased stride duration is associated with a decrease of this parameter in the baseline condition,

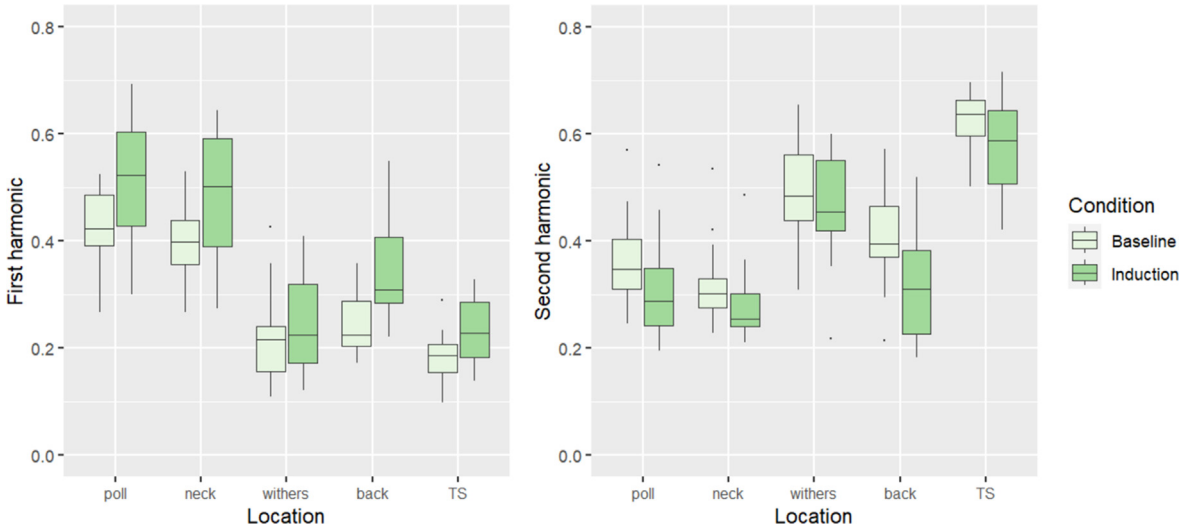

Fig. 8. Left: box plots showing the distribution of amplitudes of first harmonic of vertical displacement for the different upper body landmarks, for baseline compared to induction condition. Right: box plots showing the distribution of amplitudes of second harmonic of vertical displacement for the different upper body landmarks, for baseline compared to induction condition. Amplitude expressed as a ratio of total range of motion is given on the y-axes. Boxplots were made from cow-level averages for each condition. Significant differences between baseline and induction condition (at grand mean of stride duration) were seen for the amplitude for the first (increase, for all displayed body landmarks) and second (decrease, for all displayed body landmarks) harmonics. TS=*tubera sacrale.*

while in the induction condition, increased stride duration is associated with an increase of the outcome parameter (as the slope estimates are negative and positive, respectively). For a few outcome parameters, the effect of stride duration was significant, while the interaction between stride duration and condition was not: pro_max (non-induced limb), lat_diss (induced and non-induced limb involvement) and withers_ROMz decreased with increasing stride duration irrespective of condition. Re_max (induced limb) and back_ROMz increased with increasing stride duration irrespective of condition.

Discussion

In this study, kinematic changes in dairy cows with induced hindlimb lameness were investigated in straight line walk using 11 body-mounted IMUs. Lameness was induced, using a promptly reversible method, by external mechanical pressure to the sole of the lateral claw or to the interdigital space. Temporal and spatial limb parameters as well as spatial upper body parameters were considered, in part adopting approaches which are commonly used in the field of equine biomechanics (Serra Bragança et al., 2018) and focusing on between stride-half differences. This is, to the authors' best knowledge, the first study to investigate lameness-associated kinematic changes in cows by considering such a large number of anatomical landmarks simultaneously, thus offering a detailed picture of movement pattern alterations. Our results, which were based on data from >3 000 strides, show that many of the investigated parameters differ between baseline and induction conditions, and thus show potential as future indicators of a cow's lameness status.

The analysis of temporal limb parameters (visualised in Fig. 7) showed lameness-associated changes, where foot-on of the lame limb can be interpreted as "delayed", while the placements of the non-lame hindlimb and its ipsilateral forelimb can be interpreted as "hurried" (all relative to foot-on of the preceding limb). The distal limb angle analysis revealed lameness-associated decreases of the protraction angle of the lame limb and of the retraction angle of the non-lame limb. This does seem logic as these occur more or less simultaneously, resulting in a smaller limb spread during dual support of the hindlimbs where the lame limb is protracted, compared to the opposite situation.

Significant increases in the vertical displacements' first harmonic amplitude, and decreases in the vertical displacements' second harmonic amplitude were seen in all investigated body landmarks (poll, neck, withers, back and TS). This implies that the up- and downward excursions of these locations differed more between the two stride halves in the induction compared to the baseline condition, i.e. that the normal sinusoid-like pattern with two periods normally seen in sound animals (Loscher et al., 2016) was deranged. For the poll (and neck) and back, where the largest changes were seen, this corresponds well with the visually obvious disturbances to the vertical displacement curves. In most of the cows, the back reaches its maximum position during stance of the lame limb, while the head reaches its minimum position. During stance phase of the non-lame hindlimb, this relationship is reversed; the head is (relatively speaking) elevated, and the back is lowered. Thus, these segments seem to go from oscillating up and down twice per stride cycle (as expected in sound animals), towards only doing so once, such that the first rather than the second harmonic dominates in the induction condition, as also described in horses by Rhodin et al. (2016). For the withers and TS, the increases in vertical asymmetry were smaller, and accordingly, the sinusoid curve containing two periods per stride was generally still quite clearly discernible in the induction condition. The lameness-associated absolute increases in withers_Maxdiff and TS_Mindiff however indicate that smaller disruptions to this pattern systematically occurred in accordance with early stance phase of the lame limb, as discussed below. See Fig. 9 and supplementary Figure S2 for visualisation and further explanations.

Considering the above, interpretations of compensatory mechanisms and kinematic interrelationships of different body segments throughout the stride cycle can be made. First, the distal portion of the lame hindlimb is advanced less than its counterpart (as illustrated by a decreased metatarsal segment protraction angle) and its foot-on is "delayed" (relative to preceding foot-on of the contralateral forelimb), which can perhaps be said to reflect a reluctance to bear weight. Around this time, the withers and TS are

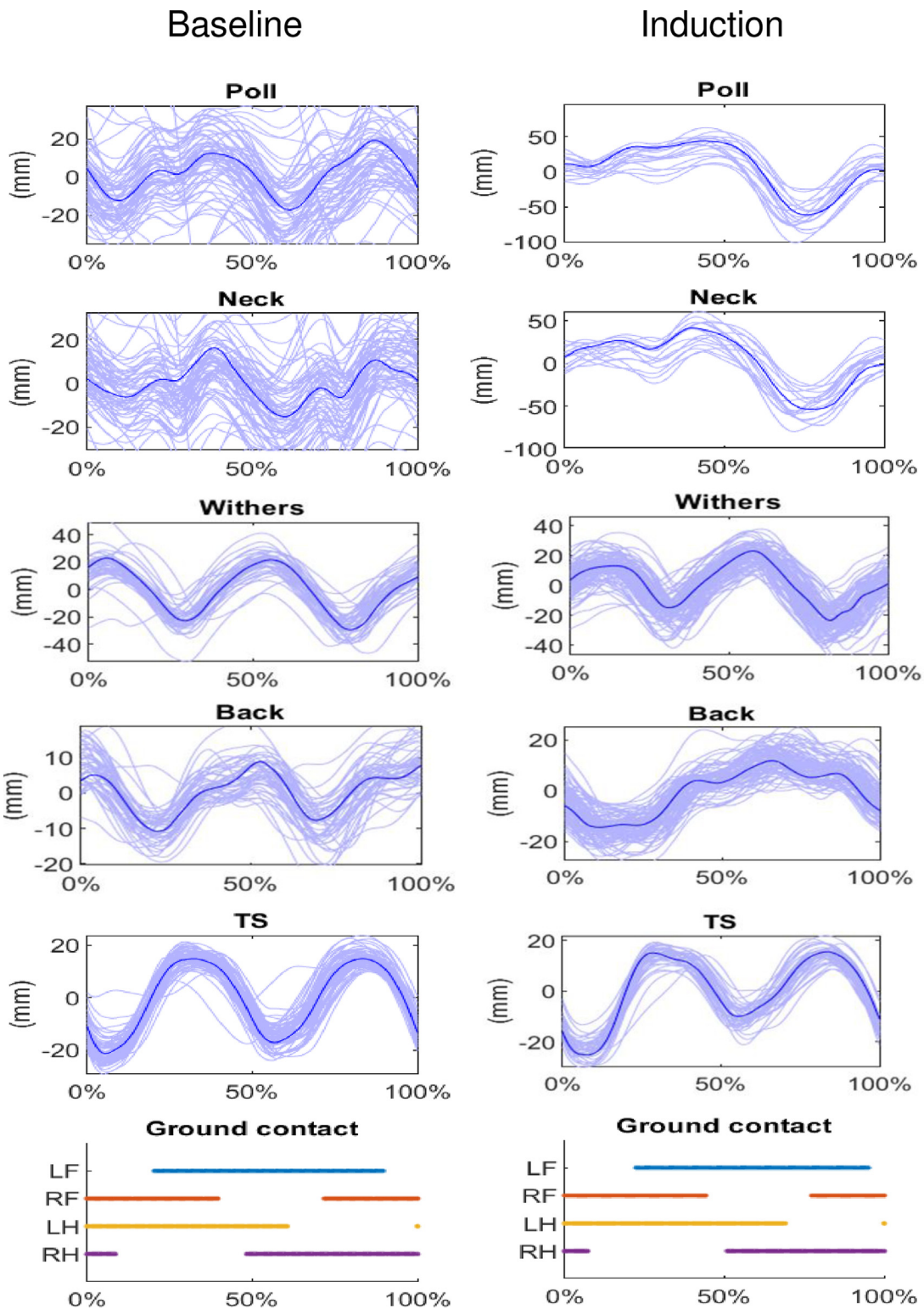

Fig. 9. Examples of vertical displacement curves for poll, neck and TS IMUs from one cow. For visualisation purposes, the vertical displacement curves of the withers and back IMUs were taken from a different cow, and the Y-axis scale was set individually for each measurement. Lameness was induced in the right hindlimb (RH) for both cows. Left: baseline measurement, right: lameness induction measurement. Most common stride for each IMU (inertial measurement unit) and measurement is shown as a dark blue line, and all remaining strides are shown as shaded blue lines. All strides are time normalised, starting at left hind (LH) foot-on. Mean stance phases are given in bottom plots, and percentage of stride is given on the X-axis of each plot. In the induction condition, the poll and neck are lowered during stance phase of the lame limb (RH), and elevated during stance of the non-lame limb (LH). The back instead reaches its maximum position during stance of the lame limb, and its minimum position during stance of the non-lame limb. Thus, in the induction condition, the double-wave sinusoid-like patterns which dominate in the baseline condition are replaced by a dominating single-wave pattern. For the withers and TS (*tubera sacrale*) IMUs, the double-wave pattern with two local maxima and minima seen in the baseline condition is still evident in the induction condition, but with increased differences between local extrema. For the withers, a higher vertical position is seen during mid-stance of left front (LF) (and early stance of the lame hindlimb, i.e. RH) compared to mid-stance of right front (RF). For the TS; a higher vertical position is seen during early stance of the lame limb (RH) compared to the non-lame limb (LH). Vertical displacement plots for all measurements can be found in Supplementary Figure S2.

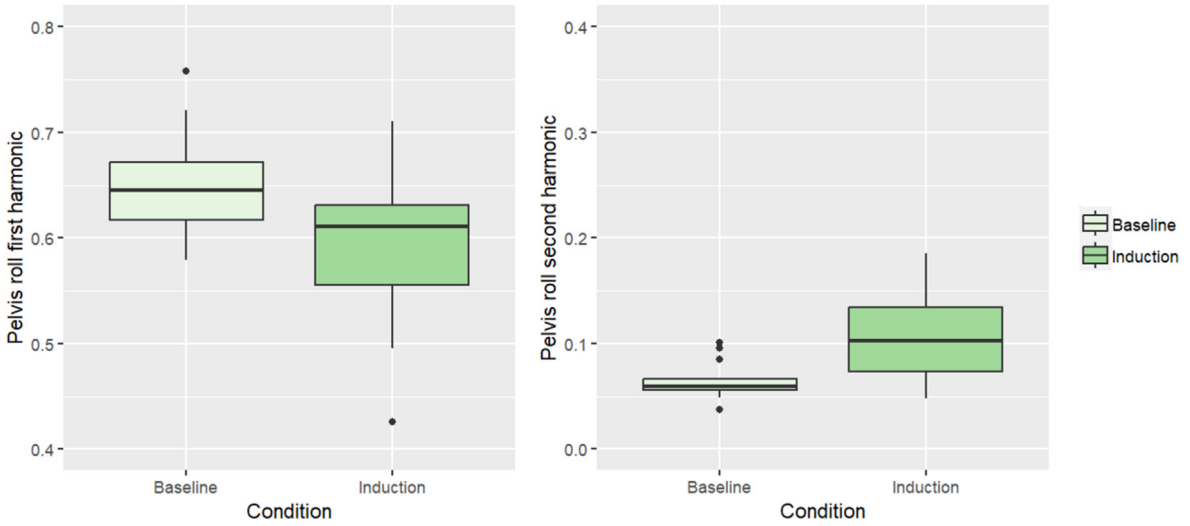

Fig. 10. Left: box plots showing the distribution of amplitudes of first harmonic of pelvic roll angle, for baseline compared to induction condition. Right: box plots showing the distribution of amplitudes of second harmonic of pelvic roll angle, for baseline compared to induction condition. Amplitude expressed as a ratio of total range of motion is given on the y-axis. Boxplots were made from cow-level averages for each condition. A significant difference between baseline and induction condition (at grand mean of stride duration) was seen both for the first (decrease) and second harmonic (increase) amplitude of pelvic roll.

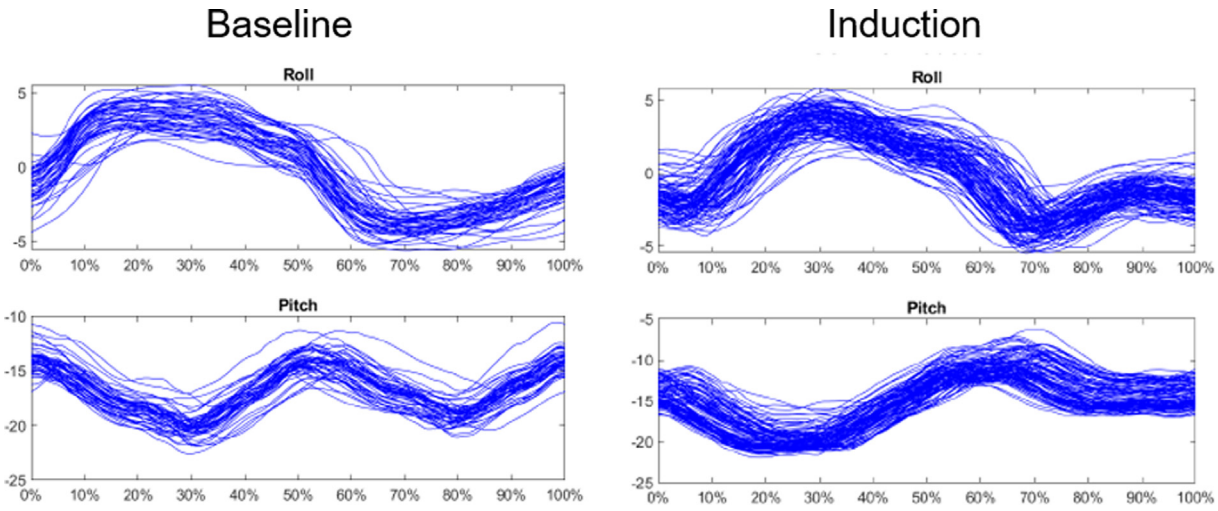

Fig. 11. Representative example of roll and pitch angle curves for one cow, with a right hindlimb (RH) lameness induction, during baseline measurement (left) and induction measurement (right). The Y-axis shows degree of rotation, and X-axis shows the percentage of stride relative to foot-on of the left hindlimb (LH). For visualisation purposes, the Y-axis scale was set individually for each measurement. All strides are time normalised, and each line represents one stride. Thus, foot-on of the right hindlimb occurs around 50%, and mid-stance/mid-swing phase of LH/RH and RH/LH occurs around 25 and 75% of the stride, respectively. Roll: maximum degrees of rotation occur around 25 and 75% of the stride, i.e. during mid-swing/mid-stance phase of each hindlimb. Pitch: in the baseline condition, peaks occur around 0, 25, 50, and 75% of each stride, i.e. around foot-on and mid-swing/mid-stance phase of each limb. In the induction condition, a more pronounced counter-clockwise rotation as seen from the right (defined as negative direction of rotation) is seen around 25% of the stride, i.e. during swing of RH (the induced limb). Roll and pitch plots for all measurements can be found in Supplementary Figure S3.

both found at a higher position compared to the corresponding phase of the opposite stride half (as indicated by changes in withers_Maxdiff and TS_Mindiff). For the TS IMU, this corresponds with the observed changes in protraction and retraction angles; a smaller hindlimb spread might logically be reflected as a higher TS position, although e.g. changes in joint angle patterns (Pluk et al., 2012) where the limb is "abnormally stiff" could also impact this, and further reflect a reluctance to bear weight on the lame limb. The higher position of the withers in this phase is reflected by the back position; through the lame limb stance, the back is (relatively speaking) elevated, and the head is lowered (as also described Zhao et al. (2023), and in horses by Gómez Álvarez et al. (2008)). Although it was not possible to obtain absolute positions in relation to the 3D space using the current IMU setup, it seems plausible that the head is truly carried closer to the ground during stance phase of the induced limb in the induction compared to the baseline condition. Lowering the head during the lame stance should contribute to transferring weight away from the painful limb, and corresponds with "head bobbing", which is described as an important attribute of lameness in cows (Flower and Weary, 2006). Subsequently, although not statistically significant ($P = 0.15$), foot-on of the forelimb ipsilateral to the lame hindlimb tends to be delayed (in relation to foot-on of the lame limb), possibly reflecting reluctance to continue to transfer weight onto the lame limb after its foot-on. Thereafter, the times before foot- on of the non-lame hindlimb (relative to the preceding foot-on of the forelimb ipsilateral to the lame hindlimb), and consecutively, its ipsilateral forelimb (relative to preceding foot-on of the

non-lame hindlimb) are both shortened. This may reflect an attempt to quickly transfer weight to the "non-lame side" of the body, and possibly also a compensatory mechanism to maintain walking speed; as stride duration was unaltered by lameness induction, absolute, and not only relative, changes in temporal parameters are implied.

When it comes to pelvic rotation, the visual appearance of the roll patterns seems to correspond with those seen in horses (Byström et al., 2023; Egenvall et al., 2023). Maximum degree of rotation in each direction is seen around the mid-swing phase of each hindlimb, which is expected as the hip of the swinging limb should be maximally "dropped" around this time. The relationship between the observed changes of the first and second harmonics is, furthermore, reversed compared to upper body vertical displacement; with lameness induction, an increase in the amplitude of the second harmonic, and a decrease in the amplitude of the first harmonic, is seen. In the induction condition, higher-frequency components hence make up a larger part of the signal than in the baseline condition, which may be due to the increased irregularities in the movement of the hindlimbs. However, the first harmonic (i.e. a sine wave oscillating with 1x stride frequency, representing the axial rotation of the pelvis which reflects the alternating steps of the hindlimbs) dominates in both conditions; see Fig. 11. Due to the chosen approach where roll was obtained from the vertical displacement of the RTC and LTC IMUs, static offset where one hip is constantly more "dropped" than the other (which has been detected in horses with hindlimb lameness by Starke and May (2021)) could not be detected; this should be kept in mind when interpreting results. For the pitch angle, maximum degrees of rotation are instead seen around the mid-swing phase (where maximum "caudal" rotation, i.e. counter-clockwise rotation as seen from the right, occurs) and foot-on (where maximum "cranial" rotation, i.e. clockwise rotation as seen from the right, occurs) of each hindlimb. The tendency (P = 0.053) towards an increased TS_pitch may be due to an increased degree of rotation during the swing phase of the lame limb in the induction condition (shown in Fig. 11). The roll and pitch angle curves are visualised and further explained in Fig. 11 and Supplementary Figure S3.

As speed is known to influence kinematic parameters (Walker et al., 2010; Weishaupt et al., 2010), stride duration and its interaction with condition were considered in our statistical analyses to improve model fit. As also indicated in (Walker et al., 2010), it seems that effects of stride duration may often be worth correcting for when obtaining kinematic measures in cows. In our data, no difference in stride duration was seen between baseline and induction conditions. This stands in contrast to previous findings (Flower et al., 2005) and might be due to the fact that most cows were only mildly lame, or that they were influenced by handlers during measurements. Further research about the effect of speed on kinematic parameters is needed.

Mechanical lameness induction methods causing transient, fully reversible lameness are commonly employed in equine research (e.g. Buchner et al., 1996; Weishaupt et al., 2004; 2006). Although not as commonly used in bovines, alteration of gait using mechanical methods has been reported in some previous studies (Haladjian et al., 2018; Cramer et al., 2023). Studying induced rather than naturally occurring lameness gives the opportunity to easily employ within-animal study designs, which is favourable as the inter-individual variability of kinematic parameters can be considerable (Telezhenko 2009; Tijssen et al., 2021). In case of undetected, concurrent pathology (Bergsten, 1994), lameness induction still guarantees increased lameness in each subject. All cows in the current study were monitored by expert assessors during and after lameness induction to ensure that only measurements where a clear, stable lameness was present, and where the induction device remained intact, were included. Thus, it was assured that the goal of the study (i.e. to compare kinematics between lame and non-lame animals) was achieved. Further research should however aim to develop improved methodological protocols that ensure a stable lameness induction with regard to e.g. choice of material and attachment technique. Despite the advantages of using mechanical lameness induction methods, follow-up studies on cows with spontaneously occurring lameness are, additionally, warranted to confirm findings, as complicating factors such as e.g. multilimb lameness can be expected in clinical lameness cases (Manske et al., 2002).

Due to the large number of IMUs and the high amount of manual labour required to obtain these results, the methods used here are not directly implementable on farms. However, our findings could serve as a basis for development of on-farm surveillance systems; in later years, great advances have been made in the field of computer vision, enabling tracking of multiple anatomical landmarks without the need for body-mounted sensors (e.g. Russello et al., 2022; Lawin et al., 2023; Barney et al., 2023). Hence, computation of kinematic parameters such as the ones presented here could potentially be implemented in video-based surveillance systems with the purpose of detecting lame animals. Furthermore, computer vision systems as well as extensive knowledge about kinematic changes associated with lameness in bovines could allow for development of direct and automatic assessment of temporal and spatial relationships between several different body landmarks so that "patterns" (rather than changes in isolated anatomical locations, which might be less informative) associated with lameness can be recognised.

Finally, some aspects regarding the chosen signal processing procedures should be mentioned. In this study, methodology was adopted from equine biomechanics, and therefore largely focusing on analysis of upper body vertical displacement. Although the analysed parameters seem highly useful as indicators of lameness also in bovines, one should be aware of the fact that at the walk, other components such as e.g. horizontal or "latero-lateral" displacement of the trunk also make up a substantial part of the motion (Serra Bragança et al., 2021), and thus potentially may provide useful information regarding a cow's lameness status. This matter should be investigated in future research. Further, fast Fourier transform was applied to signals to extract their main components, and although the first two harmonics explained most of the signals in question (and changed significantly with lameness induction), some portion was left "unexplained". Whether this portion also contains information that could help discriminate between lame and non-lame animals, and also whether different analysis strategies could be suitable, is yet to be explored.

Conclusion

In this study, we compared a large number of spatial and temporal kinematic measures in cows with and without experimentally induced hindlimb lameness, and identified several parameters which could potentially discriminate between mildly to moderately lame and sound dairy cows. In our study population, lameness caused increased asymmetry in upper body vertical displacement measures as well as in distal limb angles related to early stance phase of the lame limb. There were also changes in temporal limb parameters, pelvic rotation and vertical ROM measures. This knowledge may be useful for future development of automated, video-based surveillance systems.

Supplementary material

Supplementary material to this article can be found online at https://doi.org/10.1016/j.animal.2024.101269.

Ethics approval

This study was approved by the Swedish Ethics Committee and performed according to the Swedish legislation on animal experiments (diary number 5.8.18-10570/2019). The 3 Rs (Reduce, Refine, Replace) were considered during planning and execution of the study.

Data and model availability statement

None of the data were deposited in an official repository, but they are available upon request to the authors. The code used in statistical analyses can be found in Supplementary Material S1.

Declaration of Generative AI and AI-assisted technologies in the writing process

During the preparation of this work the author(s) did not use any AI and AI-assisted technologies.

Author ORCIDs

Anna Leclercq: https://orcid.org/0000-0002-7108-9781.
Katrina Ask: https://orcid.org/0000-0002-7336-3852.
Ylva Mellbin: https://orcid.org/0009-0006-8801-343X.
Anna Byström: https://orcid.org/0000-0002-2008-8244.
Filipe Serra Bragança: https://orcid.org/0000-0001-8514-7949.
Maja Söderlind: https://orcid.org/0009-0001-1548-1711.
Evgenij Telezhenko: https://orcid.org/0000-0001-7388-8205.
Christer Bergsten: https://orcid.org/0000-0003-0901-4698.
Pia Haubro Andersen: https://orcid.org/0000-0002-6039-7439.
Marie Rhodin: https://orcid.org/0000-0003-0575-2765.
Elin Hernlund: https://orcid.org/0000-0002-5769-3958.

CRediT authorship contribution statement

A. Leclercq: Writing – review & editing, Writing – original draft, Validation, Methodology, Investigation, Formal analysis, Data curation. **K. Ask:** Writing – review & editing, Methodology, Investigation, Data curation. **Y. Mellbin:** Writing – review & editing, Visualization, Software, Formal analysis. **A. Byström:** Writing – review & editing, Software, Methodology, Formal analysis. **F.M. Serra Bragança:** Writing – review & editing, Software, Resources, Methodology, Conceptualization. **M. Söderlind:** Writing – review & editing, Data curation. **E. Telezhenko:** Writing – review & editing, Methodology, Investigation, Conceptualization. **C. Bergsten:** Writing – review & editing, Methodology, Investigation, Conceptualization. **P. Haubro Andersen:** Writing – review & editing, Funding acquisition, Conceptualization. **M. Rhodin:** Writing – review & editing, Supervision, Resources, Funding acquisition, Conceptualization. **E. Hernlund:** Writing – review & editing, Supervision, Resources, Project administration, Funding acquisition, Conceptualization.

Declaration of interest

None.

Acknowledgements

We would like to thank the staff and animals at the Swedish Livestock Research Centre at Lövsta, Swedish University of Agricultural Science, for their contributions. We also want to thank J. Lundblad, C. Frisk and M. Tijssen for their help during data collection.

Financial support statement

This work was supported by the Swedish Research Council FORMAS (grant number 2016-01760).

References

Agriculture and Horticulture Development Board 2023. Mobility scoring: how to score your cows | AHDB. Retrieved on 4 July 2023 from: https://ahdb.org.uk/knowledge-library/mobility-scoring-how-to-score-your-cows.
Alsaaod, M., Luternauer, M., Hausegger, T., Kredel, R., Steiner, A., 2017. The cow pedogram - analysis of gait cycle variables allows the detection of lameness and foot pathologies. Journal of Dairy Science 100, 1417–1426.
Audigié, F., Pourcelot, P., Degueurce, C., Geiger, D., Denoix, J.M., 2002. Fourier analysis of trunk displacements: a method to identify the lame limb in trotting horses. Journal of Biomechanics 35, 1173–1182.
Barney, S., Dlay, S., Crowe, A., Kyriazakis, I., Leach, M., 2023. Deep learning pose estimation for multi-cattle lameness detection. Scientific Reports 13, 4499. https://doi.org/10.1038/s41598-023-31297-1.
Batens, D., Mächler, M., Bolker, B., Walker, S., 2015. Fitting linear mixed-effects models using lme4. Journal of Statistical Software 67, 1–48.
Bergsten, C., 1994. Haemorrhages of the sole horn of dairy cows as a retrospective indicator of laminitis: an epidemiological study. Acta Veterinaria Scandinavica 35, 55–66.
Bosch, S., Serra Bragança, F., Marin-Perianu, M., Marin-Perianu, R., Jan van der Zwaag, B., Voskamp, J., Back, W., van Weeren, R., Havinga, P., 2018. EquiMoves: a wireless networked inertial measurement system for objective examination of horse gait. Sensors 18, 850. https://doi.org/10.3390/s18030850.
Buchner, H.H.F., Savelberg, H.H.C.M., Schamhardtt, H.C., Barneveld, A., 1996. Head and trunk movement adaptations in horses with experimentally induced fore- or hindlimb lameness. Equine Veterinary Journal 28, 71–76.
Byström, A., Hardeman, A.M., Engell, M.T., Swagemakers, J.H., Koene, M.H.W., Serra Bragança, F.M., Rhodin, M., Hernlund, E., 2023. Normal variation in pelvic roll motion pattern during straight-line trot in hand in warmblood horses. Scientific Reports 13, 17117. https://doi.org/10.1038/s41598-023-44223-2.
Cha, E., Hertl, J.A., Bar, D., Gröhn, Y.T., 2010. The cost of different types of lameness in dairy cows calculated by dynamic programming. Preventive Veterinary Medicine 97, 1–8.
Coetzee, J.F., Mosher, R.A., Anderson, D.E., Robert, B., Kohake, L.E., Gehring, R., White, B.J., KuKanich, B., Wang, C., 2014. Impact of oral meloxicam administered alone or in combination with gabapentin on experimentally induced lameness in beef calves. Journal of Animal Science 92, 816–829.
Cramer, G., Shepley, E., Knauer, W., Crooker, B., Wagner, S., Caixeta, L., 2023. An iterative approach to the development of a sole ulcer induction model in Holstein cows. Journal of Dairy Science 106, 4932–4948.
Crecan, C.M., Peştean, C.P., 2023. Inertial sensor technologies—their role in equine gait analysis, a review. Sensors 14, 6301. https://doi.org/10.3390/s23146301.
Egenvall, A., Engström, H., Byström, A., 2023. Back motion in unridden horses in walk, trot and canter on a circle. Veterinary Research Communications 47, 1831–1843.
Egger-Danner, C., Nielsen, P., Fiedler, A., Mueller, K., Fjeldaas, T., Döpfer, D., Daniel, V., Bergsten, C., Cramer, G., Christen, A.-M., Stock, K.F., Thomas, G., Holzhauer, M., Steiner, A., Clarke, J., Capion, N., Charfeddine, N., Pryce, J.E., Oakes, E., Burgstaller, J., Heringstad, B., Ødegard, C., Kofler, J., Egger, F., Cole, J.B., 2015. ICAR Claw health atlas. ICAR Technical Series, International Committee for Animal Recording, Rome, Italy.
Engel, B., Bruin, G., Andre, G., Buist, W., 2003. Assessment of observer performance in a subjective scoring system : visual classification of the gait of cows. Journal of Agricultural Science 140, 317–333.
Espejo, L.A., Endres, M.I., Salfer, J.A., 2006. Prevalence of lameness in high-producing holstein cows housed in freestall barns in Minnesota. Journal of Dairy Science 89, 3052–3058.
Flower, F.C., Weary, D.M., 2006. Effect of hoof pathologies on subjective assessments of dairy cow gait. Journal of Dairy Science 89, 139–146.
Flower, F.C., Sanderson, D.J., Weary, D.M., 2005. Hoof pathologies influence kinematic measures of dairy cow gait. Journal of Dairy Science 88, 3166–3173.
Fox, J., Weisberg, S., 2019. An R companion to applied regression. Sage, Thousand Oaks, CA, USA.
Gómez Álvarez, C.B., Bobbert, M.F., Lamers, L., Johnston, C., Back, W., Van Weeren, P. R., 2008. The effect of induced hindlimb lameness on thoracolumbar kinematics during treadmill locomotion. Equine Veterinary Journal 40, 147–152.
Green, L.E., Hedges, V.J., Schukken, Y.H., Blowey, R.W., Packington, A.J., 2002. The impact of clinical lameness on the milk yield of dairy cows. Journal of Dairy Science 85, 2250–2256.
Haladjian, J., Haug, J., Nüske, S., Bruegge, B., 2018. A wearable sensor system for lameness detection in dairy cattle. Multimodal Technologies and Interaction 2, 27. https://doi.org/10.3390/MTI2020027.
Halekoh, U., Højsgaard, S., 2014. A Kenward-Roger approximation and parametric bootstrap methods for tests in linear mixed models – the R package pbkrtest. Journal of Statistical Software 59, 1–30.
Hildebrand, M., 1989. The quadrupedal gaits of vertebrates. Bioscience 39, 766–775.

Inertia Technology, n.d. EquiMoves - Equine Gait Analysis Using Wireless Inertial Sensor Networks - Inertia Technology. Retrieved on 16 November 2023 from: https://inertia-technology.com/project/equimoves-equine-gait-analysis-using-wireless-inertial-sensor-networks/.

Kang, X., Zhang, X., Liu, G., 2020. Accurate detection of lameness in dairy cattle with computer vision: A new and individualized detection strategy based on the analysis of the supporting phase. Journal of Dairy Science 103, 10628–10638.

Keegan, K.G., Pai, P.F., Wilson, D.A., Smith, B.K., 2001. Signal decomposition method of evaluating head movement to measure induced forelimb lameness in horses trotting on a treadmill. Equine Veterinary Journal 33, 446–451.

Keegan, K.G., Arafat, S., Skubic, M., Wilson, D.A., Kramer, J., 2003. Detection of lameness and determination of the affected forelimb in horses by use of continuous wavelet transformation and neural network classification of kinematic data. American Journal of Veterinary Research 64, 1376–1381.

Kozak, M., Piepho, H.P., 2017. What's normal anyway? residual plots are more telling than significance tests when checking ANOVA assumptions. Journal of Agronomy and Crop Science 1, 86–98.

Lawin, F.J., Byström, A., Roepstorff, C., Rhodin, M., Almlöf, M., Silva, M., Andersen, P. H., Kjellström, H., Hernlund, E., 2023. Is markerless more or less? comparing a smartphone computer vision method for equine lameness assessment to multi-camera motion capture. Animals 13, 390. https://doi.org/10.3390/ANI13030390.

Leach, K.A., Whay, H.R., Maggs, C.M., Barker, Z.E., Paul, E.S., Bell, A.K., Main, D.C.J., 2010. Working towards a reduction in cattle lameness: 1. understanding barriers to lameness control on dairy farms. Research in Veterinary Science 89, 311–317.

Leach, K.A., Tisdall, D.A., Bell, N.J., Main, D.C.J., Green, L.E., 2012. The effects of early treatment for hindlimb lameness in dairy cows on four commercial UK farms. The Veterinary Journal 193, 626–632.

Lenth, R., 2023. emmeans: Estimated Marginal Means, aka Least-Squares Means. R package version 1.8.4-1. Retrieved on 24 October 2023 from: https://CRAN.R-project.org/package=emmeans.

Lorenzini, I., Schindhelm, K., Haidn, B., Weingut, F., Koßmann, A., Reiter, K., Misha, E., 2017. Validation and comparison of two different pedometers that could be used for automatic lameness detection in dairy cows. Chemical Engineering Transactions 58, 187–192.

Loscher, D.M., Meyer, F., Kracht, K., Nyakatura, J.A., 2016. Timing of head movements is consistent with energy minimization in walking ungulates. Proceedings of the Royal Society B: Biological Sciences 283, 20161908. doi: 10.1098/rspb.2016.1908.

Maertens, W., Vangeyte, J., Baert, J., Jantuan, A., Mertens, K.C., De Campeneere, S., Pluk, A., Opsomer, G., Van Weyenberg, S., Van Nuffel, A., 2011. Development of a real time cow gait tracking and analysing tool to assess lameness using a pressure sensitive walkway: the GAITWISE system. Biosystems Engineering 110, 29–39.

Manske, T., Hultgren, J., Bergsten, C., 2002. Prevalence and interrelationships of hoof lesions and lameness in Swedish dairy cows. Preventive Veterinary Medicine 54, 247–263.

Mokaram Ghotoorlar, S., Mehdi Ghamsari, S., Nowrouzian, I., Shiry Ghidary, S., 2012. Lameness scoring system for dairy cows using force plates and artificial intelligence. The Veterinary Record 170, 126. https://doi.org/10.1136/VR.100429.

Nejati, A., Bradtmueller, A., Shepley, E., Vasseur, E., 2023. Technology applications in bovine gait analysis: a scoping review. PloS One 18, e0266287.

O'Connor, A.H., Shalloo, L., Bokkers, E.A.M., de Boer, I.J.M., Hogeveen, H., Sayers, R., Byrne, N., Ruelle, E., 2023. Modeling the economic impacts of mobility scores in dairy cows under Irish spring pasture-based management. Journal of Dairy Science 106, 1218–1232.

O'Leary, N.W., Byrne, D.T., O'Connor, A.H., Shalloo, L., 2020. Invited review: Cattle lameness detection with accelerometers. Journal of Dairy Science 103, 3895–3911.

Peham, C., Scheidl, M., 1996. A method of signal processing in motion analysis of the trotting horse. Journal of Biomechanics 29, 1111–1114.

Penell, J.C., Egenvall, A., Bonnett, B.N., Olson, P., Pringle, J., 2005. Specific causes of morbidity among Swedish horses insured for veterinary care between 1997 and 2000. Veterinary Record 157, 470–477.

Persson-Sjodin, E., Hernlund, E., Pfau, T., Andersen, P.H., Forsström, K.H., Byström, A., Serra Bragança, F.M., Hardeman, A., Greve, L., Egenvall, A., Rhodin, M., 2023. Withers vertical movement symmetry is useful for locating the primary lame limb in naturally occurring lameness. Equine Veterinary Journal 56, 76–88.

Pfau, T., Witte, T.H., Wilson, A.M., 2005. A method for deriving displacement data during cyclical movement using an inertial sensor. Journal of Experimental Biology 208, 2503–2514.

Pluk, A., Bahr, C., Poursaberi, A., Maertens, W., van Nuffel, A., Berckmans, D., 2012. Automatic measurement of touch and release angles of the fetlock joint for lameness detection in dairy cattle using vision techniques. Journal of Dairy Science 95, 1738–1748.

Posit team, 2023. RStudio: Integrated Development Environment for R. Posit Software, PBC, Boston, MA. Retrieved on 24 October 2023 from: http://www.posit.co/.

R Core Team, 2023. R: A Language and Environment for Statistical Computing. R Foundation for Statistical Computing, Vienna, Austria. Retrieved on 24 October 2023 from: https://www.R-project.org/.

Rhodin, M., Serra-Bragança, F.M., Persson-Sjodin, E., Roepstorff, L., Weishaupt, M.A., Egenvall, A., Pfau, T., 2016. Lack of a Double-Peaked Vertical Head Movement in Moderately Lame Horses with Induced Lameness. Proceedings of the 8th international conference on canine and equine locomotion, 17-19 August 2016, London, UK, p. 37.

Roepstorff, C., Dittmann, M.T., Arpagaus, S., Serra Bragança, F.M., Hardeman, A., Persson-Sjödin, E., Roepstorff, L., Gmel, A.I., Weishaupt, M.A., 2021. Reliable and clinically applicable gait event classification using upper body motion in walking and trotting horses. Journal of Biomechanics 114, 110146. https://doi.org/10.1016/J.JBIOMECH.2020.110146.

Russello, H., Van Der Tol, R., Kootstra, G., 2022. T-LEAP: occlusion-robust pose estimation of walking cows using temporal information. Computers and Electronics in Agriculture 192, 106559. https://doi.org/10.1016/j.compag.2021.106559.

Schlageter-Tello, A., Bokkers, E.A.M., Groot Koerkamp, P.W.G., Van Hertem, T., Viazzi, S., Romanini, C.E.B., Halachmi, I., Bahr, C., Berckmans, D., Lokhorst, K., 2014a. Effect of merging levels of locomotion scores for dairy cows on intra- and interrater reliability and agreement. Journal of Dairy Science 97, 5533–5542.

Schlageter-Tello, A., Bokkers, E.A.M., Koerkamp, P.W.G., Van Hertem, T., Viazzi, S., Romanini, C.E.B., Halachmi, I., Bahr, C., Berckmans, D., Lokhorst, K., 2014b. Manual and automatic locomotion scoring systems in dairy cows: a review. Preventive Veterinary Medicine 116, 12–25.

Scott, G.B., 1989. Changes in limb loading with lameness for a number of Friesian cattle. British Veterinary Journal 145, 28–38.

Serra Bragança, F.M., Bosch, S., Voskamp, J.P., Marin-Perianu, M., Van der Zwaag, B.J., Vernooij, J.C.M., van Weeren, P.R., Back, W., 2017. Validation of distal limb mounted inertial measurement unit sensors for stride detection in Warmblood horses at walk and trot. Equine Veterinary Journal 49, 545–551.

Serra Bragança, F.M., Rhodin, M., van Weeren, P.R., 2018. On the brink of daily clinical application of objective gait analysis: what evidence do we have so far from studies using an induced lameness model? Veterinary Journal 234, 11–23.

Serra Bragança, F.M., Hernlund, E., Thomsen, M.H., Waldern, N.M., Rhodin, M., Byström, A., van Weeren, P.R., Weishaupt, M.A., 2021. Adaptation strategies of horses with induced forelimb lameness walking on a treadmill. Equine Veterinary Journal 53, 600–611.

Smit, I.H., Hernlund, E., Persson-Sjodin, E., Björnsdóttir, S., Gunnarsdottir, H., Gunnarsson, V., Rhodin, M., Serra Braganca, F.M., 2023. Adaptation strategies of the Icelandic horse with induced forelimb lameness at walk, trot and tölt. Equine Veterinary Journal 56, 617–630. https://doi.org/10.1111/evj.13998.

Sprecher, D.J., Hostetler, D.E., Kaneene, J.B., 1997. A lameness scoring system that uses posture and gait to predict dairy cattle reproductive performance. Theriogenology 47, 1179–1187.

Starke, S.D., May, S.A., 2021. Robustness of five different visual assessment methods for the evaluation of hindlimb lameness based on tubera coxarum movement in horses at the trot on a straight line. Equine Veterinary Journal 54, 1103–1113.

Telezhenko, E., 2009. Measurement of spatial gait parameters from footprints of dairy cows. Animal 3, 1746–1753.

Thomsen, P.T., Shearer, J.K., Houe, H., 2023. Prevalence of lameness in dairy cows: a literature review. The Veterinary Journal 295, 1090–10233.

Thorup, V., do Nascimento, O., Skjøth, F., Voigt, M., Bennedsgaard, T., Ingvartsen, K., 2014. Short communication: Changes in gait symmetry in healthy and lame dairy cows based on 3-dimensional ground reaction force curves following claw trimming. Journal of Dairy Science 97, 7679–7684.

Tijssen, M., Serra Bragança, F.M., Ask, K., Rhodin, M., Andersen, P.H., Telezhenko, E., Bergsten, C., Nielen, M., Hernlund, E., 2021. Kinematic gait characteristics of straight line walk in clinically sound dairy cows. PLoS ONE 16, e0253479.

Toussaint-Raven, E., Haalstra, R.T., Petersen, D.J., 1989. Cattle footcare and claw trimming. Farming Press, Ipswich, UK.

Valenti, R.G., Dryanovski, I., Xiao, J., 2015. Keeping a good attitude: a quaternion-based orientation filter for IMUs and MARGs. Sensors 15, 19302–19330.

Van Nuffel, A., Saeys, W., Sonck, B., Vangeyte, J., Mertens, K.C., De Ketelaere, B., Van Weyenberg, S., 2015a. Variables of gait inconsistency outperform basic gait variables in detecting mildly lame cows. Livestock Science 177, 125–131.

Van Nuffel, A., Zwertvaegher, I., Pluym, L., Van Weyenberg, S., Thorup, V.M., Pastell, M., Sonck, B., Saeys, W., 2015b. Lameness detection in dairy cows: part 1. how to distinguish between non-lame and lame cows based on differences in locomotion or behavior. Animals 5, 838–860.

Ventura, B.A., von Keyserlingk, M.A.G., Weary, D.M., 2015. Animal welfare concerns and values of stakeholders within the dairy industry. Journal of Agricultural and Environmental Ethics 28, 109–126.

Viazzi, S., Bahr, C., Schlageter-Tello, A., Van Hertem, T., Romanini, C.E.B., Pluk, A., Halachmi, I., Lokhorst, C., Berckmans, D., 2013. Analysis of individual classification of lameness using automatic measurement of back posture in dairy cattle. Journal of Dairy Science 96, 257–266.

Walker, A.M., Pfau, T., Channon, A., Wilson, A., 2010. Assessment of dairy cow locomotion in a commercial farm setting: the effects of walking speed on ground reaction forces and temporal and linear stride characteristics. Research in Veterinary Science 88, 179–187.

Weishaupt, M.A., Wiestner, T., Hogg, H.P., Jordan, P., Auer, J.A., 2004. Compensatory load redistribution of horses with induced weightbearing hindlimb lameness trotting on a treadmill. Equine Veterinary Journal 36, 727–733.

Weishaupt, M.A., Wiestner, T., Hogg, H.P., Jordan, P., Auer, J.A., 2006. Compensatory load redistribution of horses with induced weight-bearing forelimb lameness trotting on a treadmill. The Veterinary Journal 171, 135–146.
Weishaupt, M.A., Hogg, H.P., Auer, J.A., Wiestner, T., 2010. Velocity-dependent changes of time, force and spatial parameters in Warmblood horses walking and trotting on a treadmill. Equine Veterinary Journal 42, 530–537.
Winckler, C., Willen, S., 2001. The Reliability and repeatability of a lameness scoring system for use as an indicator of welfare in dairy cattle. Acta Agriculturae Scandinavica 30, 103–107.
Zhao, K., Zhang, M., Ji, J., Zhang, R., Bewley, J.M., Ji, J., 2023. Automatic lameness scoring of dairy cows based on the analysis of head-and back-hoof linkage features using machine learning methods. Biosystems Engineering 230, 424–441.